Rab 7: An Important Regulator of Late Endocytic Membrane Traffic

Yan Feng, Barry Press, and Angela Wandinger-Ness

Department of Biochemistry, Molecular Biology and Cell Biology, Northwestern University, Evanston, Illinois 60208-3500

Abstract. Rab5 and rab7 proteins belong to a superfamily of small molecular weight GTPases known to be associated with early and late endosomes, respectively. The rab5 protein plays an important regulatory role in early endocytosis, yet the function of rab7 protein was previously uncharacterized. This question was addressed by comparing the kinetics of vesicular stomatitis virus (VSV) G protein internalization in baby hamster kidney cells overexpressing wild-type or dominant negative mutant forms of the rab7 protein (rab7N125I and rab7T22N). Overexpression of wild-type rab7 protein allowed normal transport to late endosomes (mannose 6-phosphate receptor positive), while the rab7N125I mutant caused the VSV G protein to accumulate specifically in early (transferrin receptor positive) endosomes. Horseradish peroxidase and paramyxovirus SV5 hemagglutinin-neuraminidase (HN) were used in quantitative biochemical assays to further demonstrate that rab7 function was not required for early internalization events, but was crucial in downstream degradative events. The characteristic cleavage of SV5 HN in the late endosome distinguishes internalization from transport to later stages of the endocytic pathway. Mutant rab7N125I or rab7T22N proteins had no effect on the internalization of either horseradish peroxidase or SV5 HN protein. In contrast, the mutant proteins markedly inhibited the subsequent cleavage of the SV5 HN protein. Taken together, these data support a key role for rab7, downstream of rab5, in regulating membrane transport leading from early to late endosomes. We compare our findings to those obtained for the yeast homologues Ypt51p, Ypt52p, Ypt53p, and Ypt7p.

THE late endosome represents the convergence point of numerous pathways. It is the delivery site of endocytosed material from early endosomes and of newly synthesized lysosomal proteins exiting the TGN. Endocytosed material (both fluid phase and receptor bound) is internalized in coated vesicles formed at the plasma membrane, which then fuse with and deliver their contents to the early endosomes. Here, receptors and ligands are uncoupled by the acidic pH and molecules may either recycle to the plasma membrane or be transported to the perinuclear late endosome (Goldstein et al., 1985; Yamashiro et al., 1984). In addition, there is evidence to suggest that it is the meeting point of both the autophagic route, targeting organellar and cytosolic components for destruction, and the phagocytic pathway, operative in specialized cells for the uptake of large particles (Beron et al., 1995; Desjardins et al., 1994*b*; Olkkonen et al., 1993; Rabinowitz et al., 1992). Molecules exiting the late endosome can either recycle back to the TGN, with the most notable example being the mannose 6-phosphate receptor, or they can be routed to lysosomes (Griffiths et al., 1990; Ludwig et al., 1991; Riederer et al., 1994). The latter include molecules destined to be degraded as well as molecules necessary for lysosomal function. There is also evidence for recycling to the plasma membrane from the late endosome (Riederer et al., 1994). Such a pathway may be particularly relevant in antigen-presenting cells requiring a mechanism to return major histocompatibility complex class II–antigen complexes to the cell surface after their formation in endocytic compartments (Cresswell, 1994; Germain, 1994; Qiu et al., 1994). In spite of its obvious importance in pathways leading to receptor downregulation, lysosomal enzyme delivery, antigen processing, and recycling to the Golgi apparatus, much remains unknown about late endosome function and the membrane transport pathways leading to and from the late endosome.

To address such questions one would like to be able to examine the consequences of specifically blocking transport to the late endosome. To date, this has only been possible by low temperature incubation (15°C) (Draper et al., 1984; Dunn et al., 1980, 1986) or by depolymerization of microtubules (Gruenberg et al., 1989; Oka and Weigel, 1983), both of which appear to block endocytic membrane transport leading from early to late endosomes. Since both of these treatments also affect other membrane transport steps, they are often not suitable in experiments aimed at examining interfaces between the exo- and endocytic pathways. A solution to this difficulty is afforded by the advent of dominant negative mutant rab proteins as effective tools to dissect individual membrane transport processes.

Please address all correspondence to A. Wandinger-Ness, Department of Biochemistry, Molecular Biology and Cell Biology, Hogan 2-100, 2153 North Campus Road, Northwestern University, Evanston, IL 60208-3500. Tel.: (708) 467-1173. Fax: (708) 491-2467. E-mail: w-ness@nwu.edu

The rab proteins are members of a large GTPase family (>30 known members) with homology to ras (Ferro-Novick and Novick, 1993; Novick and Brennwald, 1993; Pfeffer, 1994; Zerial and Stenmark, 1993). They are known to be important regulators of every intracellular membrane transport step examined to date (Bucci et al., 1992; Huber et al., 1993; Lombardi et al., 1993; Martinez et al., 1994; Salminen and Novick, 1987; Segev, 1991; Segev et al., 1988; Tisdale et al., 1992; van der Sluijs et al., 1992). Regulation is effected through the cyclical binding and hydrolysis of GTP. By analogy with the known structure for ras, the nucleotide bound state of the protein is believed to dictate its conformation and hence its molecular interactions (de Vos et al., 1988; Jurnak et al., 1990; Pai et al., 1989; Tong et al., 1989). Mutations within highly conserved regions (present in all family members), which disrupt this nucleotide binding and hydrolysis cycle, generally interfere with membrane traffic in a dominant negative manner (Bucci et al., 1992; Martinez et al., 1994; Plutner et al., 1991; Riederer et al., 1994; Stenmark et al., 1994; Tisdale et al., 1992; van der Sluijs et al., 1992; Walworth et al., 1989). For example, by exchanging isoleucine for asparagine in the NKXD region, the resulting rabN→I proteins fail to bind nucleotide (Bucci et al., 1992; Pind et al., 1994). Such mutant proteins were among the first to be used to demonstrate their inhibitory effect on membrane transport (Bucci et al., 1992; Tisdale et al., 1992; van der Sluijs et al., 1992; Walworth et al., 1989). More recently, substitution of leucine for glutamine in the WDTAGQE region (rabQ→L) or exchange of asparagine for serine or threonine in the GKT/S region (rabS/T→N) has generated mutants constitutively in the GTP or GDP-bound conformations, respectively (Barbieri et al., 1994; Frech et al., 1994; John et al., 1993; Li and Stahl, 1993; Nuoffer et al., 1994; Pind et al., 1994; Riederer et al., 1994; Stenmark et al., 1994; Tisdale et al., 1992). RabS/T→N mutant proteins like rabN→I have been shown to have a dominant negative effect on transport, while the rabQ→L mutant proteins have a stimulatory effect on fusion assays, but may reduce recycling. It is presumed that the mutant proteins exert their dominant effects by remaining preferentially bound to limiting membrane or cytosolic factors and interfering with the initiation of new rounds of transport. Each conformation is thought to interact with a distinct set of accessory proteins, including both effectors and regulatory molecules (Bourne et al., 1988; Bourne et al., 1990; Li et al., 1994; Pfeffer, 1994).

A number of rab proteins are associated with the endocytic pathway. Rab5 (a,b,c), rab 4 (a,b), rab18, and rab20 have all been localized to early endosomes (Lütcke et al., 1994; Simons and Zerial, 1993). Rab5 and rab4 have been characterized most extensively. It is clear that rab5a regulates the internalization of molecules via clathrin-coated vesicles and their subsequent delivery to early endosomes (Bucci et al., 1992). In addition, an in vitro early endosome fusion assay provided the first evidence that rab5a was an important regulator of homotypic fusion events between early endosomes (Gorvel et al., 1991). Overexpression of various mutant forms of rab5 protein further confirmed that rab5 was also an important regulator of early endosome fusion in vivo and that its activity in membrane fusion was stimulated by blocking its GTPase activity (Barbieri et al., 1994; Stenmark et al., 1994). Rab4 was suggested to be the counterpart of rab5 on the recycling route, regulating membrane traffic leading from early endosomes back to the plasma membrane (van der Sluijs et al., 1991, 1992).

Three rab proteins, rab7, rab9, and rab24, have been shown to be associated with late endosomes (Chavrier et al., 1990; Lombardi et al., 1993; Olkkonen et al., 1993). No rab proteins have been localized to lysosome as yet. Rab24 is also partially associated with the endoplasmic reticulum, and has therefore been speculated to be involved in autophagic processes (Olkkonen et al., 1993). Rab9 has been shown to regulate transport from the late endosome to the TGN (Lombardi et al., 1993; Riederer et al., 1994). The function of rab7, however, has previously remained uncharacterized. The yeast homologue, Ypt7p, has been alternately suggested to regulate transport from early to late endosomes (Wichmann et al., 1992) or from late endosomes to the vacuole (Schimmöller and Riezman, 1993). Given the subcellular localization of the rab7 protein, we considered it probable that it would function either in transport from early to late endosomes or alternatively in transport from late endosomes to lysosome. Therefore, we developed a series of morphological and biochemical assays which have allowed us to trace the transport of endocytic markers along the entire endocytic pathway, and have established that rab7 is an important regulator of late endocytic membrane transport leading from early to late endosomes.

Materials and Methods

Antisera, Antibodies, and Reagents

Reagents for SDS-PAGE were purchased from BioRad Laboratories (Hercules, CA), except acrylamide which was obtained from National Diagnostics (Atlanta, GA). Reagents for immunofluorescence experiments included Mowiol 4-88 from Calbiochem (La Jolla, CA); saponin, 1,4-diazabicyclo-[2,2,2]-octane (DABCO), Triton X-100, and paraformaldehyde from Sigma Chem. Co. (St. Louis, MO); all secondary antibodies and detection reagents from Vector Laboratories (Burlingame, CA); and primary antibodies from the following sources: Monoclonal I1 (8G5F11), recognizing an ectoplasmic epitope of the vesicular stomatitis virus (VSV)[1] G protein (Lefrancios and Lyles, 1982), was kindly provided by Douglas Lyles (The Bowman Gray School of Medicine, Wake Forest University, Winston-Salem, NC). Monoclonal P5D4, recognizing a cytoplasmic epitope of the VSV G protein (Kreis and Lodish, 1986), was provided by Thomas Kreis (Université de Genève, Geneva, CH). Monoclonal 4A1, recognizing hamster lysosomal glycoprotein 120, was a gift from Jean Gruenberg (Université de Genève, Geneva, CH). Monoclonal 1b, recognizing both intact and cleaved paramyxovirus SV5 HN (Ng et al., 1989; Randall et al., 1987), was generously provided by Robert Lamb (Northwestern University, Evanston, IL). Polyclonal antisera to the following antigens were kindly supplied by: Bernard Hoflack (EMBL, Heidelberg, FRG), rabbit anti-bovine mannose 6-phosphate receptor (Ludwig et al., 1991); Kathryn Howell (University of Colorado School of Medicine, Denver, CO), rabbit antisera directed against the ectoplasmic domain of VSV G protein (Gruenberg et al., 1989); Marino Zerial (EMBL, Heidelberg, FRG), rabbit anti-canine -rab5 (Chavrier et al., 1990), -rab7 (Chavrier et al., 1990), and -rab9 (Lombardi et al., 1993); and Suzanne Pfeffer (Stanford University, Stanford, CA), goat anti-human transferrin receptor. Reagents for biotinylation experiments included [^{35}S]methionine from Amersham Corp. (Arlington Heights, IL); 2-mercaptoethanesulfonic acid (MESNA) from Sigma Chem. Co.; Pansorbin® from Calbiochem; sulfo-NHS-biotin, sulfo-NHS-SS-biotin, and immobilized streptavidin from

1. *Abbreviations used in this paper*: HN, hemagglutinin-neuraminidase; MESNA, 2-mercaptoethanesulfonic acid; VSV, vesicular stomatitis virus.

Pierce Biochemical Corp. (Rockford, IL). Reagents for immunoblotting included: monoclonal 4F11 directed against the carboxy terminus of rab5 (Bucci et al., 1994) and a polyclonal antisera (R4) directed against the carboxy terminus of rab7 (Qiu et al., 1994) (these reagents were routinely used to monitor the overexpression of rab proteins by immunoblotting); HRP-conjugated antibodies and chemiluminescence detection reagents (ECL™) from Amersham Corp. Lipofectamine for transfections was obtained from GIBCO BRL (Gaithersburg, MD). Horseradish peroxidase was from Boehringer Mannheim (Indianapolis, IN). [α-^{32}P]GTP (3,000 Ci/mmol) was obtained from Amersham Corp. All other reagents were from Sigma Chem. Co. unless otherwise noted.

Cells, Cell Culture, and Transient Infection/Transfection

The baby hamster kidney, BHK21, cell line was obtained from Amer. Type Culture Collection (Rockville, MD). BHK21 cells were grown in Glasgow's modified Eagle's medium (G-MEM) supplemented with 5% FCS, 2 mM glutamine, 50 U/ml penicillin, 50 μg/ml streptomycin, and 2.6 g/ml tryptose phosphate broth at 37°C in a 5% CO_2 incubator. All tissue culture reagents were from GIBCO BRL. Cells were split 1:3 and grown for 24 h to 80% confluence, and were passaged again 18 h before transfection such that they were never more than 70–80% confluent on the day of

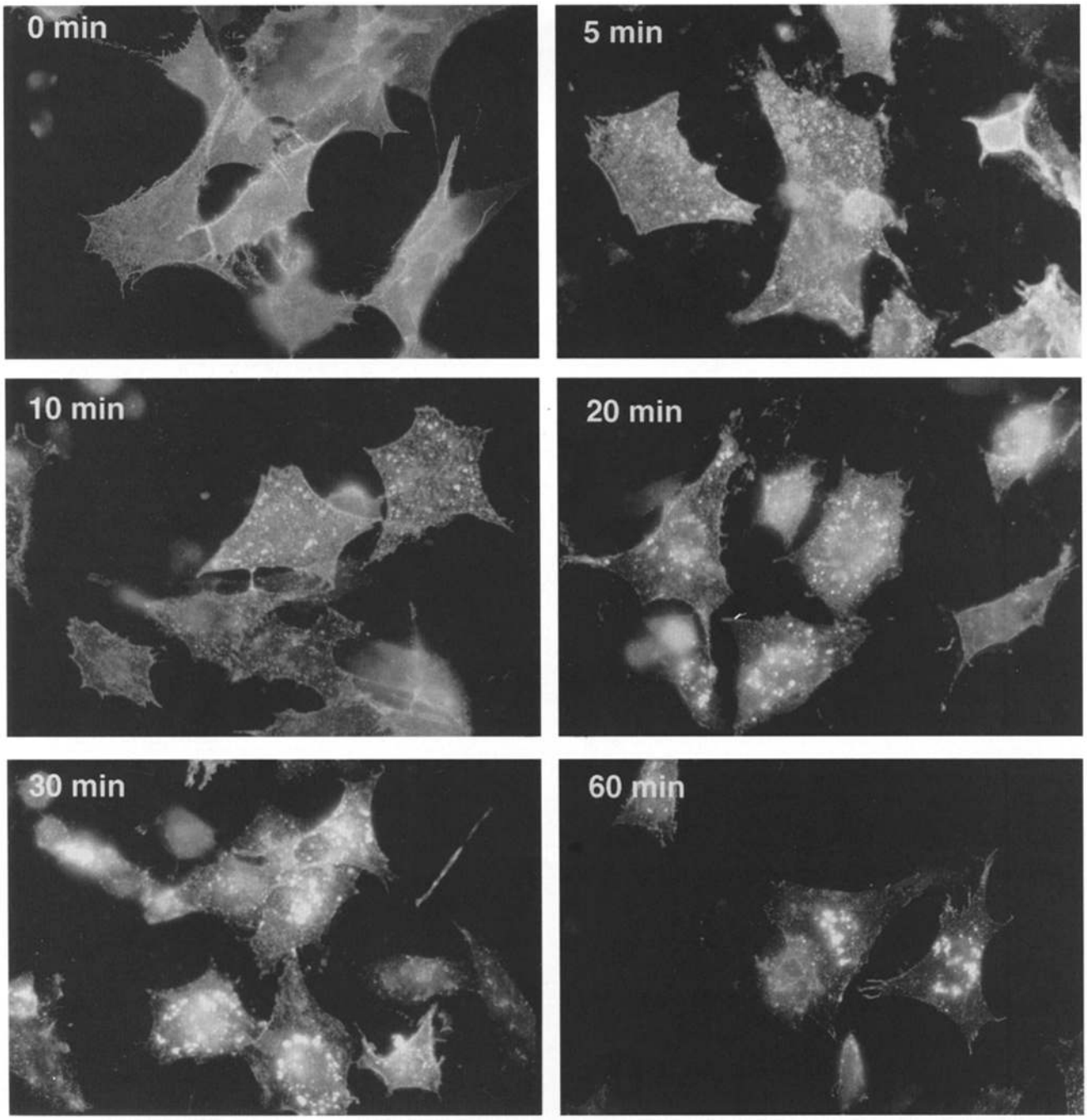

Figure 1. Kinetics of VSV G internalization. BHK cells were induced to overexpress VSV G protein using a recombinant T7 polymerase vaccinia virus infection/transfection scheme. 5 h posttransfection VSV G protein present at the cell surface was labeled by binding monoclonal I1 at 4°C. Internalization of the VSV G protein–antibody complexes was induced by returning the cells to 37°C for 0, 5, 10, 20, 30, or 60 min. At each time point samples were transferred to ice, fixed, and the internalized VSV G protein–antibody complexes were detected with an FITC labeled anti-mouse antibody. The time of internalization is noted in the upper left-hand corner of each panel.

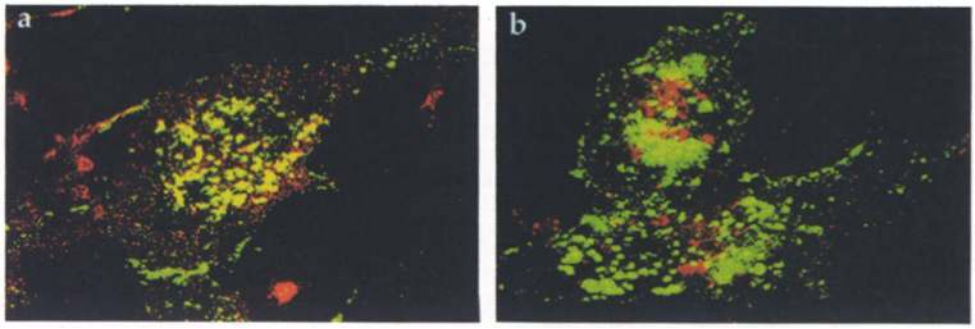

Figure 2. Colocalization of VSV G protein with late endosomes and lysosomes after 60 min of internalization. BHK cells transiently overexpressing VSV G protein were induced to internalize the protein by binding a (*a*) monoclonal I1 or (*b*) polyclonal antibody directed against VSV G protein at 4°C and subsequently rewarming cells to 37°C for 60 min. After this internalization period, cells were fixed, and processed for confocal microscopy. (*a*) Sample double stained with an FITC-labeled anti–mouse antibody to detect the VSV G protein-antibody complexes and a polyclonal antibody directed against mannose 6-phosphate receptor visualized with a (1:4) rhodamine:Texas red mixture of labeled secondary antibodies or (*b*) sample double stained with an FITC-labeled anti–rabbit antibody to detect the VSV G protein–antibody complexes and a monoclonal antibody against lgp 120 visualized with a (1:4) rhodamine:Texas red mixture of labeled secondary antibodies. The images shown represent four, 0.5 μm sections.

transfection. After washing once with serum-free medium, cells were infected with T7 RNA polymerase-recombinant vaccinia virus (vTF7.3) (Fuerst et al., 1986). Infection was carried out with 5–10 plaque forming units (p.f.u.) cell at 37°C for 30 min with occasional agitation. Cells were then washed twice with serum-free medium, and transfected with plasmids containing cDNA under the control of the bacteriophage T7 promoter using Lipofectamine reagent according to the manufacturer's instructions (GIBCO BRL); 1 μg DNA/9 μl lipofectamine. The pAR-G and pGEMrab7 plasmids were transfected at a ratio of 0.3:0.7. The total amount of DNA used in each transfection was held constant and control samples were transfected with pGEM3 vector lacking an insert.

Recombinant proteins were first detected 3 h posttransfection and reached significant levels by 5–6 h with no differences seen ± hydroxyurea (Bucci et al., 1992). For all experiments, infected/transfected cells were routinely incubated for 5–6 h at 37°C in a 5% CO_2 incubator. Under these conditions, more than 90% of the BHK cells were observed to overexpress the exogenous proteins (VSV G protein, SV5 HN, wild-type or mutant rab 5, rab7, and rab9 proteins) as monitored by immunofluorescence (see Fig. 4).

Plasmids encoding wild-type (pAR-G) (Whitt et al., 1989) and temperature-sensitive forms (pGtsO45-2/T7) (Gallione and Rose, 1985) of VSV G-protein were kindly provided by John Rose (Yale University, New Haven, CT) and Marino Zerial, respectively. Plasmids encoding rab5 (Chavrier et al., 1990), rab5N133I (Gorvel et al., 1991), rab7 (Chavrier et al., 1990), rab7N125I, rab9 (Lombardi et al., 1993), and rab9N124I were the kind gift of Marino Zerial. Rab7T22N was generated by PCR mediated site-directed mutagenesis using the following primer: GITGGTAAGAACTCACTCATGAACC (changed bases are underlined). The nucleotide sequence was confirmed using the Sequenase system (USB, Cleveland, OH). The plasmid pGEM3-HN encoding SV5 HN (Ng et al., 1989; Paterson et al., 1985) was a gift from Robert Lamb.

GTP Ligand Overlay Blotting

Sf9 cells were infected with recombinant baculoviruses encoding wild-type rab7, rab7T22N, or rab7N125I proteins. Cells were lysed in SDS-PAGE sample buffer and the proteins were resolved on 12.5% polyacrylamide gels (10 μg total protein/lane). Subsequently, proteins were transferred to nitrocellulose membranes (Schleicher and Schuell, Keene, NH) in 10 mM CAPS [3-(cyclohexylamino)-propanesulfonic acid] (Calbiochem), pH 11 containing 5% methanol, using a Genie blotter (Idea Scientific, Minneapolis, MN) at 500 mA for 30 min. Immediately after transfer the membrane was incubated in Blot buffer (50 mM sodium phosphate, pH 7.5, 10 μM $MgCl_2$, 0.3% Tween 20, 2 mM DTT, 4 μM ATP) for 30 min at room temperature, and then probed with 1 μCi/ml [α-^{32}P]GTP in Blot buffer for 2 h. After six 2-min washes with Blot buffer, the blot was wrapped wet and exposed to film. The same blot was stripped to remove the bound [α-^{32}P]GTP and reprobed with anti-rab7 antibodies as described below.

VSV G Protein Internalization Assay

BHK cells were grown on 15-mm square coverslips in 35-mm dishes (for immunofluorescence staining experiments) and transfected as described above with pAR-G to induce overexpression of VSV G protein. After a 5–6 h incubation at 37°C, cells were transferred to ice and quickly washed with ice cold serum-free medium. An excess of polyclonal antiserum or monoclonal I1 directed against the ectoplasmic domain of VSV G protein was added and cells were incubated at 4° for 30 min. The unbound antibodies were removed by washing cells three times on ice with cold serum-free medium. Subsequently, cells were warmed up to 37°C for various lengths of time to allow internalization of the VSV G-antibody complexes. Cells were then permeabilized and fixed for immunofluorescence staining. VSV G-antibody complexes were visualized by staining with either Texas red- or FITC-conjugated secondary antibodies.

Immunofluorescence Microscopy

BHK cells were grown on 15-mm square coverslips for 18 h before use. Cells were washed once with PBS^- and permeabilized with 0.5% saponin (Sigma) in 80 mM Pipes-KOH (pH 6.8), 5 mM EGTA, 1 mM $MgCl_2$ for 5 min. Cells were then fixed with 3% paraformaldehyde in PBS^+ for 15 min at room temperature. After fixation cells were washed with 0.5% saponin in PBS^+ for 5 min, and free aldehyde groups were quenched with 50 mM NH_4Cl in PBS^+ for 10 min. Cells were washed with 0.5% saponin in PBS for 5 min, and then incubated with the primary antibody in PBS containing 0.5% saponin for 20 min. The anti-rab antibodies could be used to detect only the overexpressed protein with little to no contribution of endog-

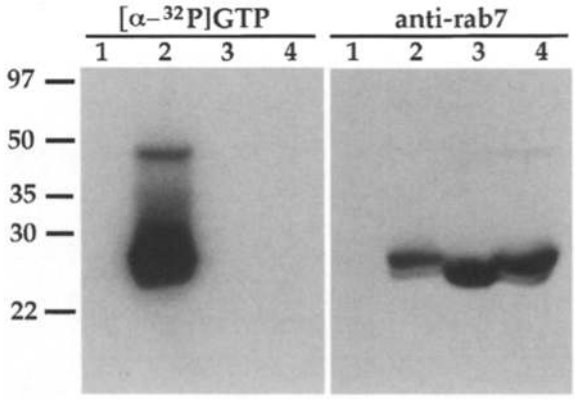

Figure 3. GTP-binding activity of rab7 wild-type and mutant proteins. Whole cell lysates were prepared from Sf9 cells which were left (*1*) uninfected or infected with recombinant baculoviruses encoding (*2*) wild-type rab7, (*3*) rab7N125I, or (*4*) rab7T22N. The proteins were resolved by SDS-PAGE, transferred to nitrocellulose and probed with radiolabeled GTP ([α-^{32}P]GTP, 1–4). After stripping the same blot was reprobed with rab7 specific antibodies (anti-rab7, 1–4) as a control for equal protein loading.

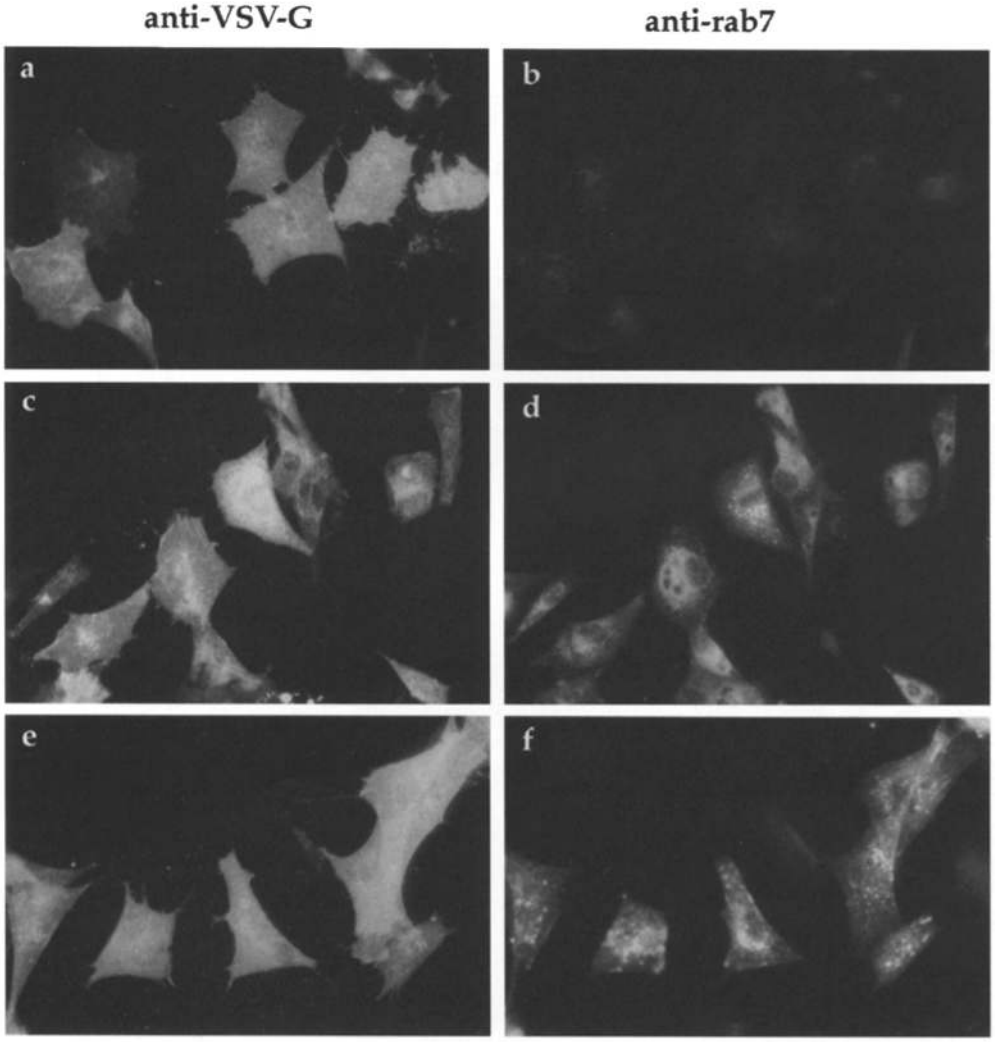

Figure 4. Coexpression of VSV G protein with Rab7 wild-type and mutant proteins. BHK cells were cotransfected with a plasmid encoding VSV G protein and either (*a–b*) a control (pGEM lacking an insert) plasmid, (*c–d*) a plasmid encoding wild-type rab7, or (*e–f*) a plasmid encoding rab7N125I as described in Materials and Methods. (*a, c,* and *e*) VSV G protein was detected with monoclonal I1, followed by an FITC-labeled anti–mouse antibody. (*b, d,* and *f*) Overexpressed rab7 proteins were visualized using an affinity-purified polyclonal anti-rab7 antibody (diluted to detect only the overexpressed rab7 protein, note that no staining was observed in the control sample [*b*] expressing only endogenous rab7 protein), followed by a Texas red labeled anti–rabbit antibody.

enous protein staining by using a dilution 50-fold greater than that required to detect the endogenous protein (Fig. 4) (Bucci et al., 1992). After rinsing cells three times with 0.5% saponin in PBS (5 min/each), they were incubated with goat anti–rabbit Texas red or horse anti–mouse FITC in PBS containing 0.5% saponin for 20 min to allow detection of primary antibody binding. Cells were then washed once with PBS containing 0.5% saponin and three times with PBS (5 min/each). The coverslips were then mounted on glass slides in Mowiol 4-88 (Calbiochem) and viewed with a Zeiss Axiophot fluorescence microscope. For double immunofluorescence, the secondary antibodies were added sequentially such that any cross-reactivity was minimized.

Confocal Microscopy and Digital Imaging

For confocal analysis, cells were fixed and stained as above, except that a mixture of goat anti–rabbit rhodamine to goat anti–rabbit Texas red (1:4) was used as a detection reagent to provide an optimal signal in the rhodamine channel with no cross-over from the FITC channel. Cells were then postfixed with 4% paraformaldehyde in PBS^+ for 30 min and quenched with 50 mM NH_4Cl in PBS^+. The coverslips were mounted on glass slides in PBS containing 50% glycerol and 1 mg/ml DABCO. For long-term storage and to prevent evaporation, the edges were sealed with nail polish. Confocal imaging was performed using a Zeiss confocal microscope (fitted with an Ar laser with a band at 488 nm for FITC and an He-Ne laser with a band at 543 nm for rhodamine) and a 63× (1.4 NA) oil immersion lens (Zeiss). A series of 0.5 μm sections was collected along the z-axis of each sample. Each image was 512 × 512 pixels and extended focus images were produced using the image processing package on the Zeiss confocal. Images were transferred as .tiff files to Adobe Photoshop where individual sections were combined and colorized before printing on a Tektronix Phaser 440 color printer.

Immunoprecipitation and Immunoblotting

BHK cells grown on 35-mm dishes were lysed in 500 μl RIPA buffer (1% NP-40, 0.5% deoxycholate, 0.1% SDS, 50 mM Tris-HCl, pH 7.4, 150 mM NaCl) with 1 mM PMSF added fresh. The lysate was incubated for 1 h on ice with a 1:1 mixture of monoclonal anti-VSV G antibodies I1 and P5D4. A polyclonal rabbit anti–mouse antibody was subsequently added, and incubation continued for 1 h followed by Pansorbin for an additional hour coupled with occasional vortexing. The immune complexes were collected by centrifugation, washed once with RIPA buffer, and then three times with high salt RIPA buffer (500 mM NaCl), and twice more with RIPA buffer. For analysis, samples were heated to 95°C for 5 min in SDS-PAGE sample buffer (50 mM Tris-HCl, pH 6.8, 2.5 mM EDTA, 2% SDS, 7% glycerol and 0.01% bromophenol blue), and separated on 10% SDS-polyacrylamide gels.

For immunoblot analysis, samples separated on 10% SDS-polyacrylamide gels were transferred onto a PVDF (Millipore, Bedford, MA) membrane. The membrane was blocked for 1 h with 3% newborn-calf serum in TBS-T (150 mM NaCl, 20 mM Tris-HCl, pH 7.4 and 0.1% Tween-20), and then probed according to manufacturer's instructions (ECL™, Amersham).

Exocytosis of VSV G Protein

BHK cells were seeded and infected with vTF7.3 as described above. After 30 min cells were transfected with pGtsO45-2/T7, a construct encoding a temperature-sensitive mutant form of VSV G protein, and incubated at 39°C for 5 h. Under these conditions VSV G tsO45 protein accumulated in the ER (de Silva et al., 1990). To monitor the kinetics of VSV G tsO45 protein transport to the cell surface, the cells were transferred to permissive temperature, 31°C, for various lengths of time and subsequently sub-

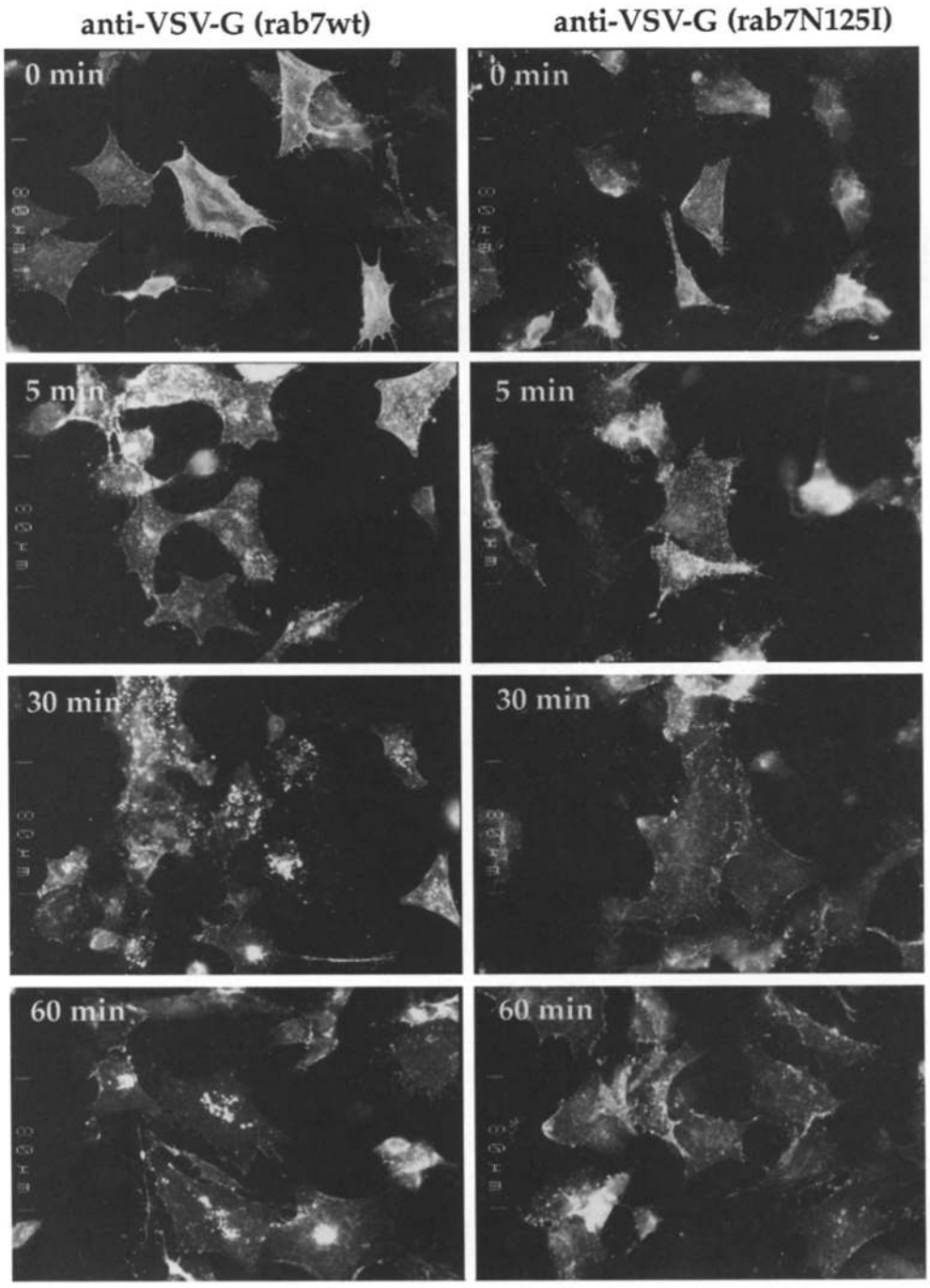

jected to surface biotinylation as detailed below. For analysis, cells were lysed in 500 μl RIPA buffer and 20 μl of the lysate was reserved and used to analyze the total VSV G and rab7 content by immunoblotting. 250 μl lysate was subjected to immunoprecipation with a mixture of anti-VSV G antibodies as outlined in the previous section to recover the VSV G tsO45 protein. The immunoprecipitates were boiled in 40 μl of 10% SDS to release bound VSV G tsO45 protein. Each sample was diluted with 400 μl Solubilization buffer and incubated for 60 min at 4°C with streptavidin-Sepharose (Pierce) to precipitate the biotinylated VSV G tsO45 protein. The biotinylated VSV G tsO45 protein was released from the streptavidin-Sepharose by boiling in SDS-PAGE sample buffer, resolved by SDS-PAGE on 10% gels, and transferred to PVDF membranes. The amount of VSV G tsO45 protein or rab7 protein in each fraction was quantified by immunoblotting with monoclonal P5D4 and polyclonal R4, respectively.

HRP Internalization and Activity Measurements

BHK cells grown on 6-cm dishes were transfected with the plasmids encoding wild-type or mutant rab7 proteins for 5 h. Cells were washed quickly three times with warm serum free GMEM. Serum free GMEM containing 5 mg/ml HRP was added to each plate (1 ml/each) and the cells were transferred to 37°C for times ranging from 1–15 min. At the end of each time point the cells were transferred to ice and washed with 4 ml/dish as follows: quickly three times with cold PBS^+/0.1% BSA, 5 min with PBS^+/10% serum, 1 min with PBS^+/1% serum, five times 30 s with PBS^+/0.1% BSA, rinse PBS^+. The cells were scraped from the dish in 1 ml PBS/0.1% Triton X-100. HRP activates were measured by diluting 100 μl of each postnuclear supernatant to a final volume of 1 ml in Reaction Buffer (50 mM sodium phosphate, pH 5, 0.1% Triton X-100, 0.1% peroxide, 0.1

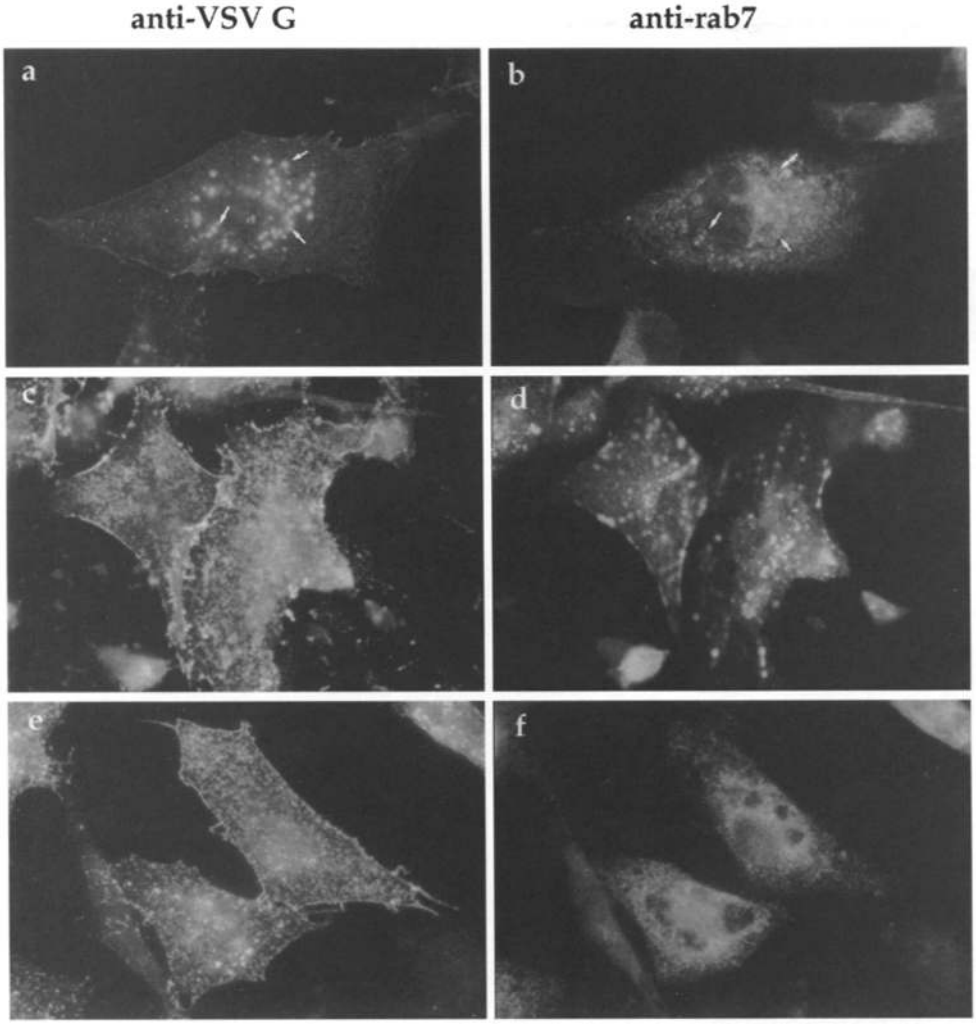

Figure 5. Rab7N125I and Rab7T22N act as dominant negative inhibitors of VSV G transport to late endosomes and lysosomes. (*A*) Wild-type rab7 (*rab7wt*) or rab7N125I mutant (*rab7N125I*) proteins were coexpressed with VSV G protein in BHK cells, as described in Materials and Methods. The kinetics of VSV G protein internalization was monitored as in Fig. 1 (using monoclonal I1) and individual time points between 0 and 60 min are shown. The VSV G protein–antibody complexes were detected with a Texas red–labeled anti–mouse antibody. (*B*) (*a–b*) Wild-type rab7, (*c–d*) rab7N125I, or (*e–f*) rab7T22N proteins were coexpressed with VSV G protein in BHK cells. Representative samples after 60 min VSV G protein internalization were stained for (*a, c,* and *e*) VSV G protein or (*b, d,* and *f*) overexpressed rab7 protein.

mg/ml o-dianisidine) and incubating the reactions for 10 min at room temperature. Reactions were stopped by the addition of 20 μl 4% sodium azide and OD measured at 460 nm. The total amount of protein was determined using BioRad DC protein assay (BioRad Labs.).

Cell Surface Biotinylation

Sulfo-NHS-biotin or sulfo-NHS-SS-biotin stock solutions (100 mg/ml in DMSO) were stored at −20°C and were diluted to 1 mg/ml in PBS, pH 8.5 containing 1 mM $MgCl_2$ and 1 mM $CaCl_2$ just before use. All reactions and washes were conducted with cells on ice in a 4°C room using ice cold solutions. BHK cells were washed twice with PBS^+ (PBS containing 1 mM $MgCl_2$ and 1 mM $CaCl_2$) before addition of 0.5 ml of the diluted biotinylation reagent. Cells were incubated three times for 10 min with fresh biotinylation reagent and agitation and subsequently the reaction was quenched by incubating with 50 mM glycine in PBS^+ twice for 10 min each. Cells were then washed three times with PBS^+. In the cases where sulfo-NHS-SS-biotin was used to biotinylate cell surface proteins, the subsequent treatment with the reducing agent MESNA resulted in efficient removal of cell surface biotin. This was accomplished by treating cells three times 30 min with 20 mM MESNA in 50 mM Tris-HCl (pH 8.6) containing 100 mM NaCl, 0.2% (wt/vol) BSA, 1 mM $MgCl_2$, and 1 mM $CaCl_2$ (Smythe et al., 1992).

SV5 HN Protein Internalization Assay

BHK cells were grown on 35-mm dishes and transfected as above with the construct encoding the SV5 hemagglutinin-neuraminidase (HN) gene. After a 4.5-h incubation at 37°C, cells were washed once with warm methionine-free medium and incubated in the same medium for an additional 30 min at 37°C. Cultures were then metabolically labeled by incubating with 0.5 ml [^{35}S]methionine (100 μCi/ml) containing medium for 30 min at 37°C. Incorporation of radioactive label was terminated by adding medium containing 100-fold excess of unlabeled methionine and cells were incubated for one additional hour at 37°C. The HN protein present at the cell surface was labeled with sulfo-NHS-SS-biotin at 4°C as described above. Cells were then returned to 37°C for various lengths of time to allow HN internalization. A control group was maintained at 4°C throughout. At the end of the incubation period, one group of cells was treated with MESNA as described above while one group was left untreated. The disulfide-linked biotin label on the cell surface was sensitive to MESNA treatment, enabling us to distinguish between intracellular and cell surface pools. For analysis, cells were transferred to ice, washed quickly with cold PBS^+, and lysed through the addition of 500 μl RIPA buffer (1% NP-40, 0.5% deoxycholate, 0.1% SDS, 50 mM Tris-HCl, pH 7.4, 150 mM NaCl) with 1 mM PMSF added fresh. HN was immunoprecipitated with monoclonal 1b and immune complexes were recovered using Pansorbin®. The precipitates were boiled in 40 μl 10% SDS to release the immunoprecipitated HN protein for analysis. One-fifth of this volume was analyzed directly by SDS-PAGE and the remainder of each sample was diluted with 400 μl Solubilization buffer (10 mM Tris-HCl, pH 8.0, 5 mM EDTA, 150 mM NaCl, 1% Triton X-100, 0.2% BSA) and incubated for 60 min at 4°C with streptavidin-Sepharose to precipitate the biotinylated HN. The biotinylated HN was released from the streptavidin-Sepharose by boiling in SDS-PAGE sample buffer and analyzed by SDS-PAGE on 10% polyacrylamide gels. The internalization of HN and the appearance of specific degradation fragments were detected by autoradiography.

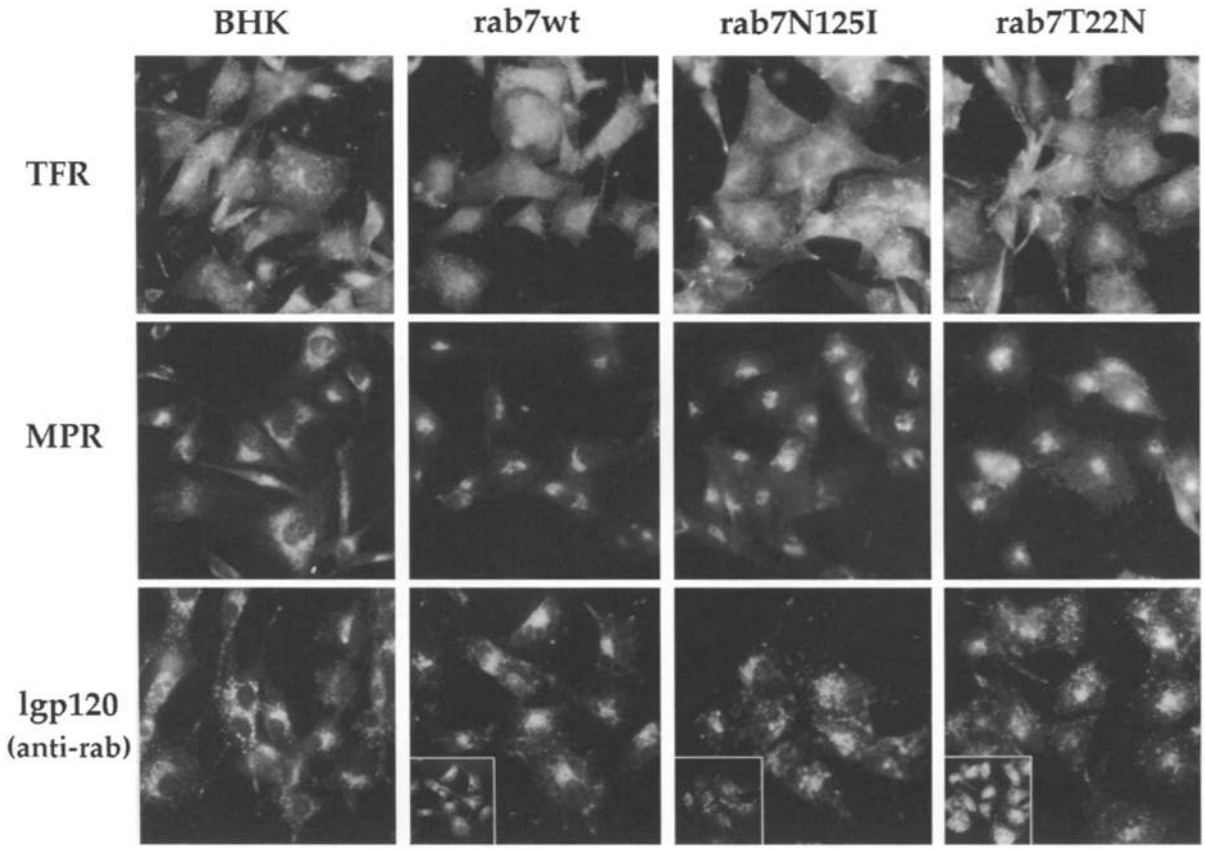

Figure 6. Distribution of endocytic markers in cells overexpressing dominant negative mutant forms of rab7. Untransfected control cells (*BHK*) and cells overexpressing wild-type rab7 (*rab7wt*) or the mutant forms (*rab7N125I, rab7T22N*) were fixed 6 h posttransfection. Replicate samples were stained with antibodies specific for transferrin receptor (*TFR*), mannose 6-phosphate receptor (*MPR*), and lysosomal glycoprotein 120 (*lgp120*). Transfection efficiencies in all cases were >90% as confirmed by staining with antibodies specific for rab7 (*anti-rab, inset panels*).

Quantification of SV5 HN Internalization and Cleavage

Quantification of ^{35}S-labeled samples was accomplished by exposing gels to phosphoimager plates and analyzing the photo-stimulated luminescence on a Fuji Bioimager equipped with MacBas software. The formulas for determining the percentages of SV5 HN biotinylated, internalized, and cleaved are as follows: % Biotinylated HN=$\{[B_{HN} + (B_{frag.} \times 66/34)]1.25/[T_{HN} + (T_{frag.} \times 66/34)]5\}$, where biotinylated ($B$) and total ($T$) values for intact SV5 HN (HN) (66-kD) and the 34-kD cleavage fragment (Frag.) were quantified from the corresponding B and T lanes (representative gel shown in Fig. 11 *C*) without (−) MESNA treatment. % Internalized HN = $\{[B_{HN} + (B_{frag.} \times 66/34)]1.25/[T_{HN} + (T_{frag.} \times 66/34)]5\}$/ % Biotinylated HN, where biotinylated (B) and total (T) values for intact SV5 HN (HN) and the 34-kD cleavage fragment (Frag.) were quantified from the corresponding B and T lanes (Fig. 11 *C*) with (+) MESNA treatment. % Internalized HN Cleaved = $\{B_{frag.} \times 66/34)/[B_{HN} + (B_{frag.} \times 66/34)]\}$, where biotinylated ($B$) values for intact SV5 HN (NH) and the 34-kD cleavage fragment (Frag.) were quantified from the corresponding B lanes (Fig. 11 *C*) with (+) MESNA treatment.

Results

VSV G Protein as an Endocytic Transport Marker

To assess the in vivo function of rab7 in endocytic membrane transport, an endocytic marker which would allow tracing of the pathway leading from the cell surface to lysosomes was required. VSV G protein was selected for this purpose for several reasons. Most importantly, previous work had shown that the synchronous transport of VSV G protein to lysosomes could be triggered by antibody mediated cross-linking of the protein at the cell surface (Gruenberg et al., 1989). In addition, expression of high levels of the cell surface VSV G protein in a manner compatible with the simultaneous overexpression of wild-type and mutant forms of rab7 was possible. Finally, the detection of VSV G protein was readily possible using numerous, available monoclonal antibodies (Kreis and Lodish, 1986; Lefrancios and Lyles, 1982).

Transient overexpression of recombinant VSV G protein was achieved by infecting BHK cells with a recombinant vaccinia virus expressing T7 RNA polymerase (Fuerst et al., 1986) and subsequent transfection with a plasmid encoding VSV G protein (Whitt et al., 1989) under the control of the T7 promoter (Fuerst et al., 1986). VSV G protein was readily detectable at the cell surface 5–6 h posttransfection and accessible to a monoclonal antibody added at 4°C (Fig. 1, *0 min*). Transfer of the cells to 37°C initiated VSV G protein internalization and the internalized complexes were detected by the addition of a labeled secondary antibody after fixation. The fact that the VSV G protein remained in a stable association with the antibody throughout the 60-min time course (shown in Fig. 1) was confirmed by demonstrating that surface-biotinylated VSV G protein colocalizes with the anti-VSV G antibody over the entire time course (data not shown). After 5 min

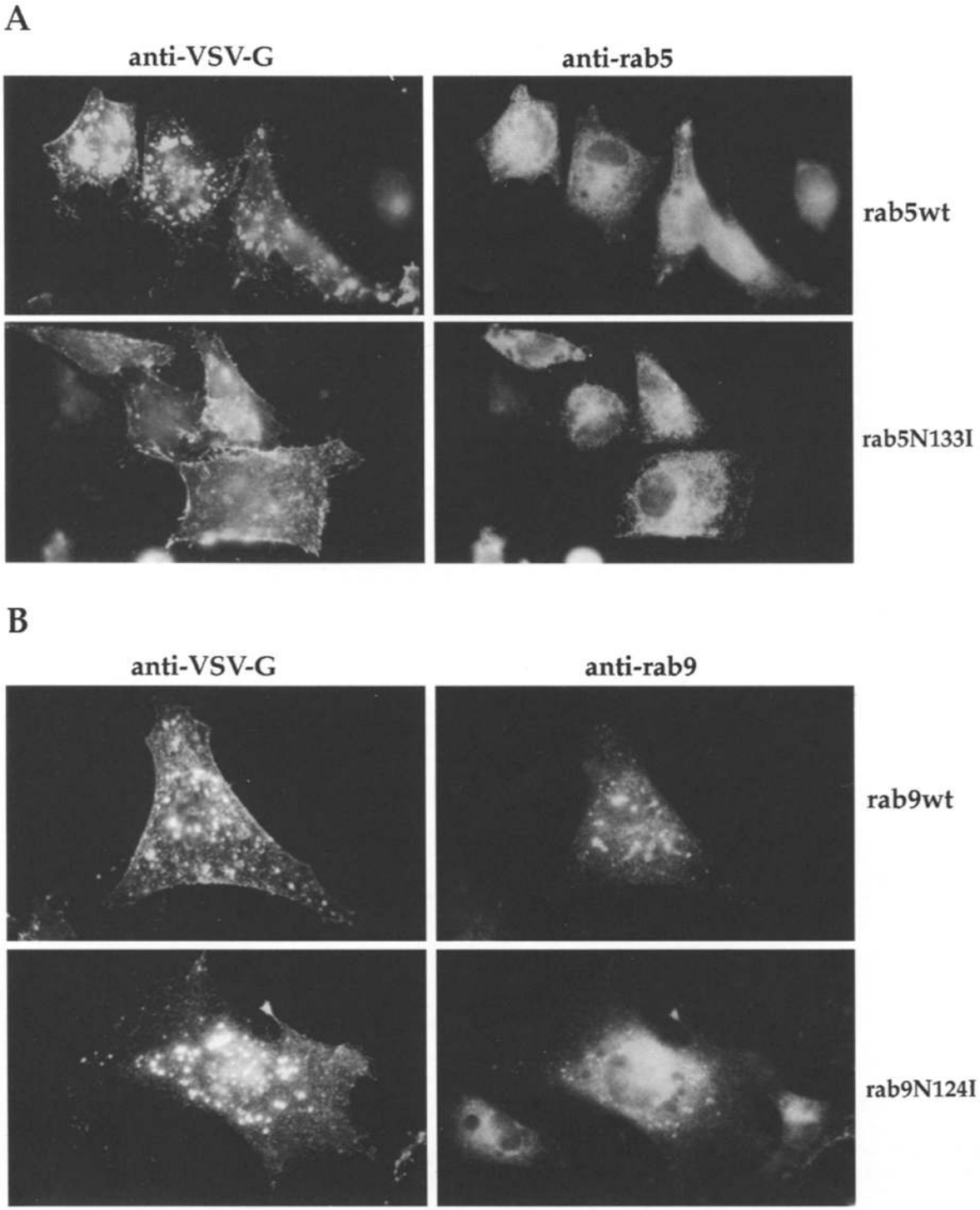

Figure 7. Effect of other endocytic Rab proteins on the transport of VSV G protein to late endosomes. (*A*) Wild-type rab5 (*rab5wt*) or mutant rab5N133I and (*B*) wild-type rab9 (*rab9wt*) or mutant rab9N124I were coexpressed with VSV G protein in BHK cells. Cells were induced to internalize the VSV G protein by binding monoclonal I1 at 4°C and subsequently rewarming the cells to 37°C for 60 min. The localization of internalized VSV G protein–antibody complexes was monitored after fixation using Texas red–conjugated anti–mouse antibody (*left-hand panels*). The overexpressed rab proteins were detected using specific polyclonal antisera to: (*A*, *right-hand panels*) rab5 and (*B*, *right-hand panels*) rab9 proteins (diluted to reveal only the overexpressed proteins) followed by an FITC-conjugated anti–rabbit antibody.

the VSV G protein–antibody complexes were detected in small, disperse endosomes underlying the cell surface (Fig. 1, *5 min*). Progressively, the internalized VSV G protein–antibody complexes were transported to later endocytic structures characterized by their perinuclear localization (Fig. 1, *10–30 min*). After 60 min, the VSV G protein–antibody complexes were exclusively localized to these perinuclear endocytic structures (Fig. 1, *60 min*). At this

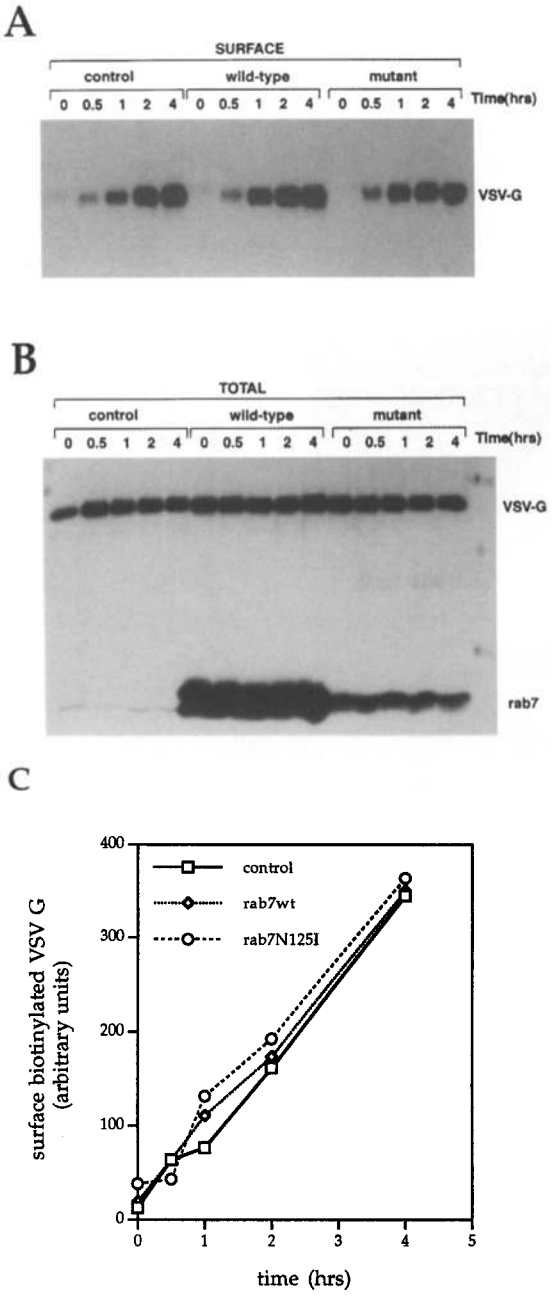

Figure 8. Exocytosis is unaffected by the overexpression of wild-type or mutant rab7 proteins. Wild-type rab7 or rab7N125I mutant proteins were coexpressed with the temperature-sensitive VSV G tsO45 protein in BHK cells. Cells were maintained at 39°C (nonpermissive temperature) for 5 h to allow accumulation of VSV G protein in the ER. Subsequently, cells were shifted to 31°C (permissive temperature) for 0, 0.5, 1, 2, and 4 h. (*A*) The cell surface delivery of VSV G tsO45 protein as a function of time was monitored by surface biotinylation as described in Materials and Methods. (*B*) A measure of the total VSV G tsO45 and rab7 protein present in the lysates was obtained by immunoblotting with monoclonal P5D4 (anti-VSV G protein) and polyclonal R4 (anti-rab7 protein). (*C*) Densitometric quantification of the cell surface appearance of VSV G protein shown in *A*.

60-min time point the VSV G protein–antibody complexes were found to be substantially colocalized with the late endosomal marker, mannose 6-phosphate receptor (Griffiths et al., 1990; Klumperman et al., 1993; Ludwig et al., 1991) (Fig. 2 *a*), and to a small extent with the lysosomal marker, lysosomal glycoprotein (lgp) 120 (Harter and Mellman, 1992; Honing and Hunziker, 1995) (Fig. 2 *b*). Degradation of the antibody and the VSV G protein in lysosomes precluded detection of greater colocalization after delivery to lysosomes even after longer incubation times. Since rab7 was known to be localized to the late endosome (Chavrier et al., 1990), it was expected that it would be involved in transport to or from this compartment. Therefore, the time course of VSV G protein internalization shown in Fig. 1 was considered suitable for the study of rab7 function in vivo.

Mutant Rab Proteins Exhibit Altered GTP Binding

Two mutants were generated each bearing a single amino acid substitution in conserved regions of rab7. The mutant rab7N125I was generated by site-directed mutagenesis, predicated on the knowledge that the analogous mutation in ras (N116I) results in a protein which acts as a dominant negative inhibitor, on account of its reduced guanine nucleotide–binding activity (Der et al., 1986; Feig et al., 1986; Sigal et al., 1986). The rab7T22N mutant was generated by substituting N for T in the GKT/S region. In ras, this mutation alters the coordination of the Mg^{2+} required for GTP binding (Milburn et al., 1990; Schlichting et al., 1990), and analogous substitutions in other rab proteins lead to the accumulation of the protein in the GDP-bound conformer (Li and Stahl, 1993; Pind et al., 1994). Ligand overlay blotting with [α-^{32}P]GTP revealed that, as expected, both mutant proteins exhibited a marked reduction in GTP binding relative to the wild-type protein (Fig. 3).

Concomitant Overexpression of VSV G Protein and Wild-Type or Mutant Rab7 Proteins

The simultaneous overexpression of VSV G protein and wild-type or mutant rab7 (rab7N125I) was achieved by cotransfecting cells with plasmids containing the corresponding cDNAs under the control of the T7 promoter (Fuerst et al., 1986). Under the conditions used, greater than 90% of the cells were transfected (Fig. 4 and data not shown). Plasmids encoding wild-type or rab7N125I proteins were cotransfected in a 2.3-fold excess over pAR-G to ensure that all cells expressing VSV G protein would also overexpress the rab7 proteins. Fig. 4 illustrates that this is the case. The rab7 proteins were overexpressed up to 50-fold above endogenous levels. Similar transfection efficiencies and overexpression levels were obtained for rab7T22N (data not shown and Fig. 6, *inset panel*). Staining with highly dilute antibody precluded detection of the endogenous protein allowing only overexpressed protein to be monitored (see Fig. 4).

Rab7N125I and Rab7T22N Act as Dominant Negative Inhibitors of VSV G Protein Transport to Late Endosomes

To investigate the function of rab7 protein in endocytosis, the wild-type protein or mutant rab7N125I or rab7T22N

proteins were overexpressed in BHK cells, and their influences on VSV G protein internalization were monitored. The internalization of VSV G protein was not dramatically altered upon overexpression of the wild-type rab7 protein (Fig. 5 *A, left hand panels* and 5 *B*, panel *a*). After a 60-min incubation period the bulk of the VSV G protein was present in the perinuclear late endosomes. In contrast, overexpression of the mutant rab7N125I protein dramatically inhibited the transport of internalized VSV G protein to the perinuclear late endosomes (Fig. 5 *A, right hand panels* and 5 *B*, panel *c*). As a result, the protein remained at the cell surface and in disperse, peripheral endosomes even after a 60-min incubation period at 37°C. Similarly, the rab7T22N mutant protein also acted as a dominant negative inhibitor, blocking transport to late endosomes (Fig. 5 *B*, panel *e*).

Each sample was costained with anti-rab7 antibodies to allow definitive identification of transfected cells. Representative samples at the 60-min time point showing the double staining with anti-VSV G protein and anti-rab7 antibodies are shown in Fig. 5 *B*. VSV G protein staining was seen to overlap at least in part with the rab7 positive endosomes when wild-type rab7 protein was overexpressed, (Fig. 5 *B*, panels *a–b*). However, this was not the case upon overexpression of the mutant proteins (Fig. 5 *B*, panels *c–f*).

Distribution of Endocytic or Lysosomal Markers Is Unaffected by Short-Term Overexpression of Wild-Type or Dominant Negative Mutant Rab7 Proteins

Conceivably the observed block in VSV G protein transport, induced by the overexpression of the rab7 mutant proteins, might be the consequence of either a failure to form late endosomes and lysosomes or a failure of molecules in transit to reach their destination. A failure to form late endosomes and lysosomes would be expected to cause a redistribution or even the disappearance of markers typically associated with late endosomes and lysosomes. If, on the other hand, rab7 merely interferes with the delivery of molecules in transit the distribution of other endocytic markers would be relatively unaffected. To address this issue, normal and transfected BHK cells overexpressing wild-type or mutant rab7 proteins were stained with antibodies against transferrin receptor (early endosome marker), mannose 6-phosphate receptor (late endosome marker), or lgp120 (lysosomal marker). The results illustrated in Fig. 6 show that there are no dramatic alterations in the distributions of any of the markers tested 6 h posttransfection. Under these experimental conditions, the exogenous rab7 proteins are known to be overexpressed at high levels beginning at 3.5 h posttransfection. Therefore, it appears that short-term overexpression of dominant negative mutant rab7 proteins does not lead to the disappearance of identifiable late endosomes and lysosomes.

Specificity of the Membrane Transport Block Induced by Overexpression of Dominant Negative Mutant Rab7 Proteins

To confirm that the effects of the dominant negative mutant rab7 proteins on VSV G protein internalization were indeed specific, a number of control experiments were conducted. First, the delivery of VSV G protein to perinuclear late endosomes after 60 min at 37°C was examined upon overexpression of wild-type and mutant forms of two other rab proteins associated with the endocytic pathway, rab5 and rab9 (Bucci et al., 1992; Lombardi et al., 1993). Upon overexpression of the wild-type rab5 and rab9 proteins, transport of VSV G protein was normal (Fig. 7 *A* and *B*, respectively). The mutant rab5N133I protein caused the VSV G protein to remain largely at the cell surface (Fig. 7 *A*), as expected given the demonstrated role of rab5 in regulating uptake from the cell surface (Bucci et al., 1992). Thus, rab5 and rab7 both appear to affect the endocytic route leading from the cell surface. On the other hand, rab9, which together with rab7 is localized to late endosomes, has been shown to regulate transport from late endosomes to the *trans*-Golgi network (Lombardi et al., 1993; Riederer et al., 1994). Hence, overexpression of mutant rab9N124I would not be expected to affect the internalization of the VSV G protein. This was indeed the case as shown in Fig. 7 *B*.

The effect of rab7N125I on the exocytosis of VSV G protein was also examined as an additional control for specificity. For this purpose cells were cotransfected with a temperature-sensitive mutant form, VSV G tsO45 (Gallione and Rose, 1985). At the nonpermissive temperature of 39°C, this protein is synthesized, but is not properly assembled and hence accumulates in the endoplasmic reticulum (Doms et al., 1987). The subsequent return of cells to the permissive temperature of 31°C allows assembly and results in the synchronous transport of the VSV G tsO45 protein to the cell surface (Doms et al., 1987), permitting the kinetics of cell surface transport to be measured.

The kinetics of VSV G tsO45 protein transport to the cell surface was measured in cells coexpressing wild-type rab7 or rab7N125I by transferring cells to the permissive temperature of 31°C for increasing lengths of time. Subsequent cell surface biotinylation was used to demonstrate a linear increase in cell surface appearance of VSV G tsO45 between 30 and 240 min (Fig. 8, *A* and *C*), which was unchanged irrespective of whether wild-type rab7 or rab7N125I was overexpressed as much as 50-fold (Fig. 8 *B*). The total amount of VSV G tsO45 protein expressed was found to be similar in all samples examined (Fig. 8 *B*).

The results of these control experiments suggest that the inhibition of VSV G protein transport to late endosomes induced by rab7N125I is indeed specific, affecting only this membrane transport step and not other endocytic or exocytic membrane transport events.

Overexpression of Dominant Negative Mutant Rab7 Proteins Causes VSV G Protein to Accumulate in Early Endosomes

Both rab7N125I and rab7T22N behaved as dominant negative mutants and blocked VSV G protein transport to the perinuclear late endosomes, suggesting that rab7 might regulate transport from early to late endosomes. If this is indeed the case, the transport marker would be expected to accumulate in early endosomes upon overexpression of the mutant proteins. To demonstrate this definitively, we took advantage of the fact that incubation of cells at 15°C allows internalization of markers into early endosomes but prevents transport to late endosomes (Draper et al., 1984;

Dunn et al., 1980, 1986). As shown in Fig. 9 *A* (panel *a*), internalized VSV G protein colocalizes exclusively with transferrin receptor, a marker of early endosomes, in cells incubated at 15°C for 1 h. Little or no VSV G protein can be detected in mannose 6-phosphate receptor positive late endosomes (Fig. 9 *A*, panel *b*). However, upon transfer of the cells back to 37°C for 30 min, the VSV G protein exits the transferrin receptor positive early endosomes (Fig. 9 *A*, panel *c*) and significantly colocalizes with mannose 6-phosphate receptor positive late endosomes (Fig. 9 *A*, panel *d*).

Upon overexpression of wild-type or mutant rab7N125I proteins, VSV G protein can be seen to accumulate in disperse early endosomes when the cells are maintained at 15°C (Fig. 9 *B*, panels *a*, and *e*). However, a dramatic difference is observed when these cells are subsequently transferred back to 37°C (Fig. 9 *B*, panels *b*, and *f*). In cells overexpressing the wild-type rab7 protein, VSV G protein is transported to the larger perinuclear late endosomes within 30 min (Fig. 9 *A*, panel *d* and Fig. 9 *B*, panel *b*), while in cells overexpressing the mutant rab7N125I protein, the VSV G protein remains in the peripheral early endosomes (Fig. 9 *B*, panel *f*). Thus, rab7 does not appear to regulate internalization into early endosomes, but rather serves to regulate a later event, transport from early to late endosomes.

Double staining with anti-rab7 antibody was used to confirm overexpression of the wild-type or mutant rab7 proteins in all cells shown (Fig. 9 *B*, panels *c–d, g–h*). The fact that rab7 was highly overexpressed and it most likely recycles between early endosomes, carrier vesicles, and late endosomes, made colocalization with VSV G protein difficult. Therefore, we used colocalization of VSV G protein with transferrin receptor or M6PR as indicators of its early or late endosomal localization.

Rab7 Function Is Not Required for Early Internalization Events but Is Crucial for Later Degradative Events

Data thus far presented would suggest that rab7 functions downstream of rab5. To prove this more directly, biochemical assays measuring the effects of rab7 on early or late endocytic events were employed. HRP was used to monitor the kinetics of fluid phase internalization. Additionally, SV5 HN, a paramyxovirus envelope protein, was used as an integral membrane transport marker to monitor both internalization and subsequent degradation events.

BHK cells overexpressing wild-type rab7 or rab7N125I proteins were monitored for their capacity to internalize the fluid phase marker HRP as compared to uninfected

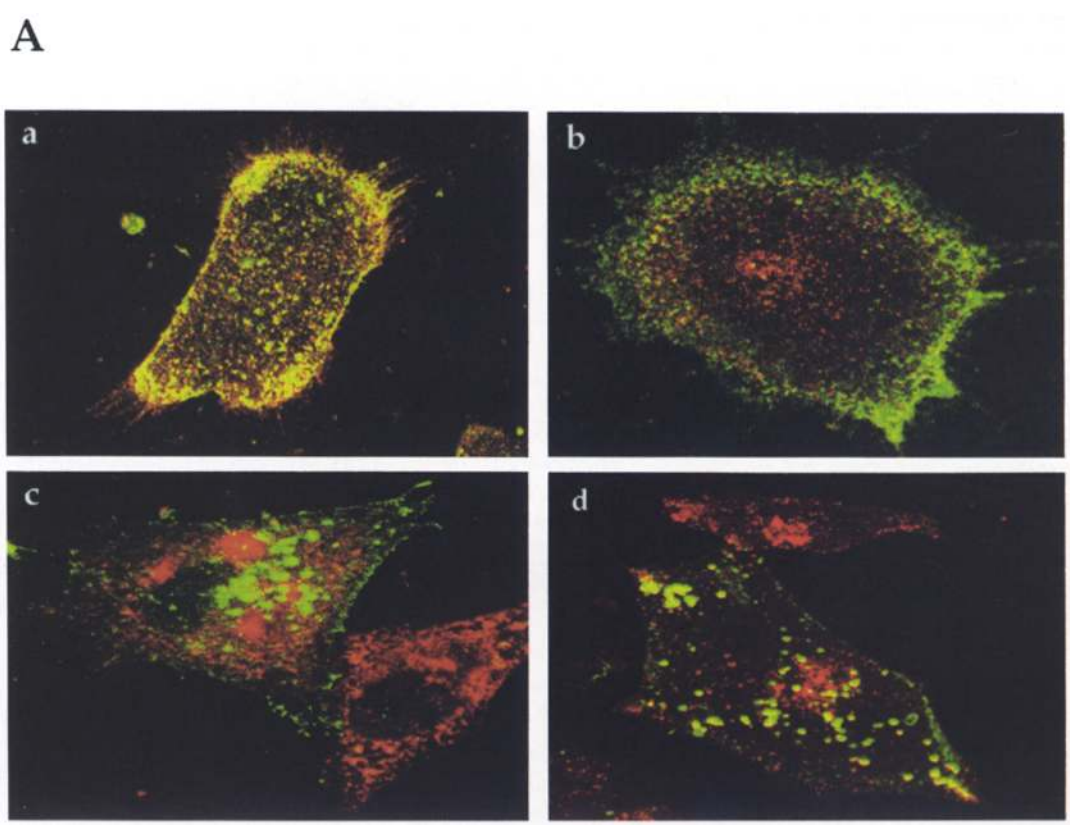

Figure 9. VSV G protein accumulates in early endosomes upon overexpression of mutant rab7N125I. VSV G protein was overexpressed in BHK cells alone or together with wild-type rab7 or rab7N125I proteins. Cells were induced to internalize the VSV G protein by binding monoclonal I1 at 4°C and subsequently rewarming the cells to 15°C for 60 min. At the end of this time, cells were either transferred directly to 4°C or first returned to 37°C for 30 min. Cells were then fixed and stained. (*A*) Confocal images of samples double stained with an FITC-labeled anti-mouse antibody to visualize VSV G protein–antibody complexes and (*a,* and *c*) a polyclonal antibody directed against transferrin receptor (rhodamine) to identify early endosomes or (*b*, and *d*) a polyclonal antibody against mannose 6-phosphate receptor (rhodamine) to identify late endosomes. Each image shows a 1-μm section. (*a–b*) Cells overexpressing only VSV G pro-

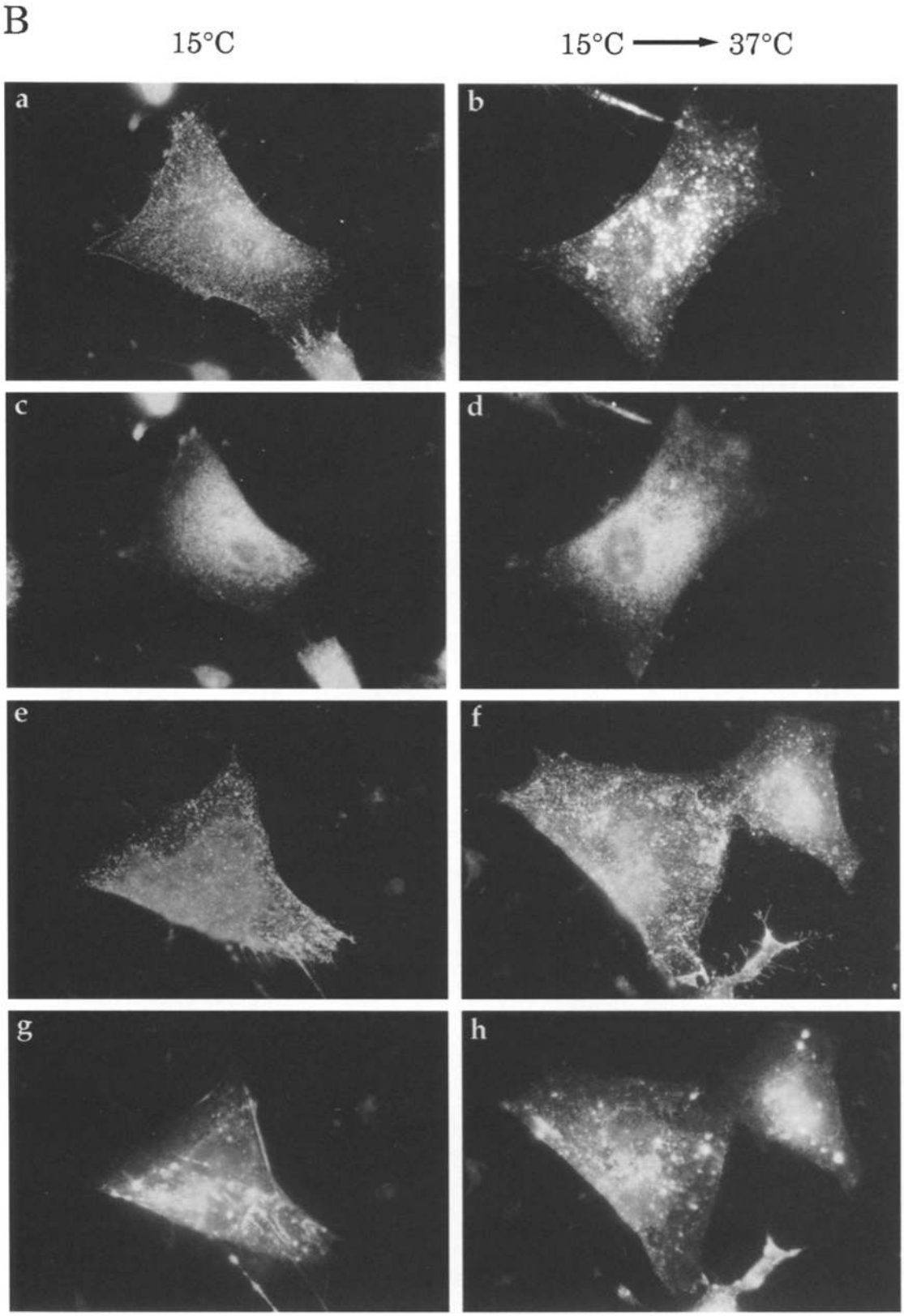

tein and maintained at 15°C for 60 min. (*c–d*) Cells overexpressing both VSV G protein and wild-type rab7 returned to 37°C for 30 min. (*B*) Cells overexpressing VSV G protein and (*a–d*) wild-type rab7 or (*e–h*) rab7N125I. The samples shown in the left hand panels were processed for fluorescence microscopy immediately after the 60-min incubation period at 15°C. The samples shown in the right hand panels were returned to 37°C for 30 min, immediately after the 15°C incubation and before fixation. Panels *a–b*, and *e–f* show VSV G protein localization and panels *c–d* and *g–h* overexpressed rab7 protein staining.

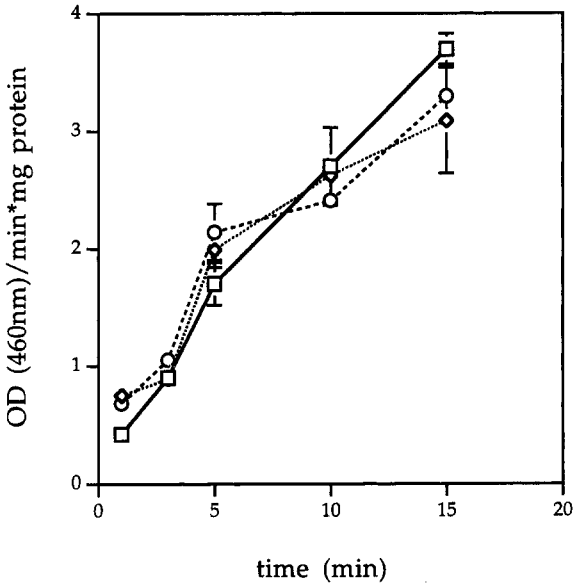

Figure 10. Rab7 does not affect the kinetics of short-term HRP internalization. Mock-transfected cells (*square*) and cells overexpressing wild-type rab7 (*diamond*), or rab7N125I (*circle*) were allowed to consititutively internalize HRP for varying lengths of time and were subsequently processed as detailed in Materials and Methods. The HRP activities of individual samples were measured and normalized to protein concentration. Each data point shown for cells overexpressing rab7 represents the average value of 4–6 independent trials and includes the SD. The data points shown for mock-transfected cells represent the average of two independent trials.

control cells. The kinetics of short term HRP internalization were found to be identical in all cases (Fig. 10). For further confirmation, experiments were performed using SV5 HN as a transport marker.

SV5 HN has the advantage over VSV G protein that it is internalized into coated vesicles even in the absence of antibody cross-linking (Ng et al., 1989). In addition, the protein is cleaved upon internalization, transiently giving rise to two distinct cleavage products which can be detected by available antibodies (Randall et al., 1987). These fragments are completely degraded after longer internalization periods (Ng et al., 1989). The kinetics of SV5 HN degradation are consistent with the notion that the cleavage fragments are formed in the late endosomes and complete degradation ensues upon delivery to lysosomes (Ng et al., 1989).

The cloned SV5 HN gene (Paterson et al., 1985) was used to overexpress the protein in a manner analogous to that used for the VSV G protein. BHK cells overexpressing SV5 HN in conjunction with wild-type or mutant rab5 and rab7 proteins were metabolically labeled and subjected to cell surface biotinylation at 4°C using NHS-SS-biotin as described under Materials and Methods. Under the conditions used ~10% of the total ^{35}S-labeled HN could be biotinylated (data not shown). After biotinylation, the cells were transferred to 37°C for 1 h and a control group was maintained at 4°C for the same period. This time point was selected since the reported $t_{1/2}$ for the degradation of HN is ~75–90 min (Leser et al., 1996). At the end of this time period, lysates were prepared from samples ± treatment with the reducing agent MESNA (cleave cell surface accessible NHS-SS-biotin) and the SV5 HN protein in each sample was recovered by immunoprecipitation. The fraction of biotinylated SV5 HN protein was quantified by subsequently isolating the biotinylated protein on streptavidin agarose. Thus, both the total and the internalized biotinylated SV5 HN protein could be quantified. In addition, since the antibody recognized both the intact and a cleaved form of the protein, it was possible to distinguish between factors affecting internalization and those affecting degradation. A more detailed description of the experimental design is given under Materials and Methods.

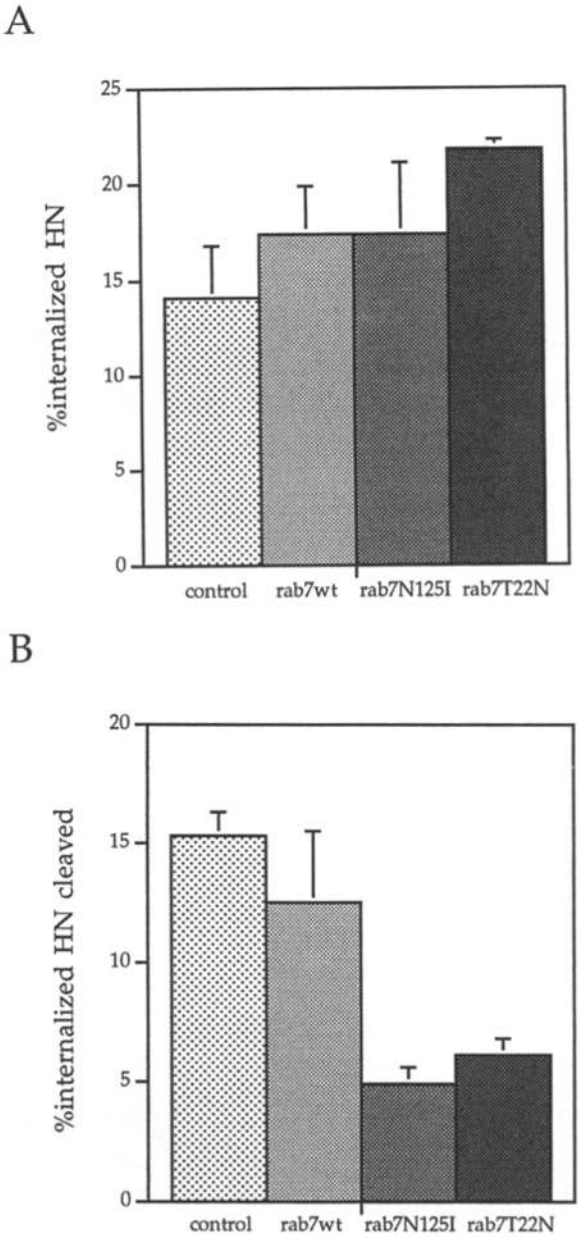

Fig. 11 shows the results of such biotinylation experiments. In the absence of warming to 37°C after biotinylation, little to no biotinylated SV5 HN was detected intracellularly (data not shown). In contrast, upon warming to 37°C for 1 h up to 23% of the cell surface biotinylated HN was internalized (Fig. 11 *A*). Cleavage of HN was also

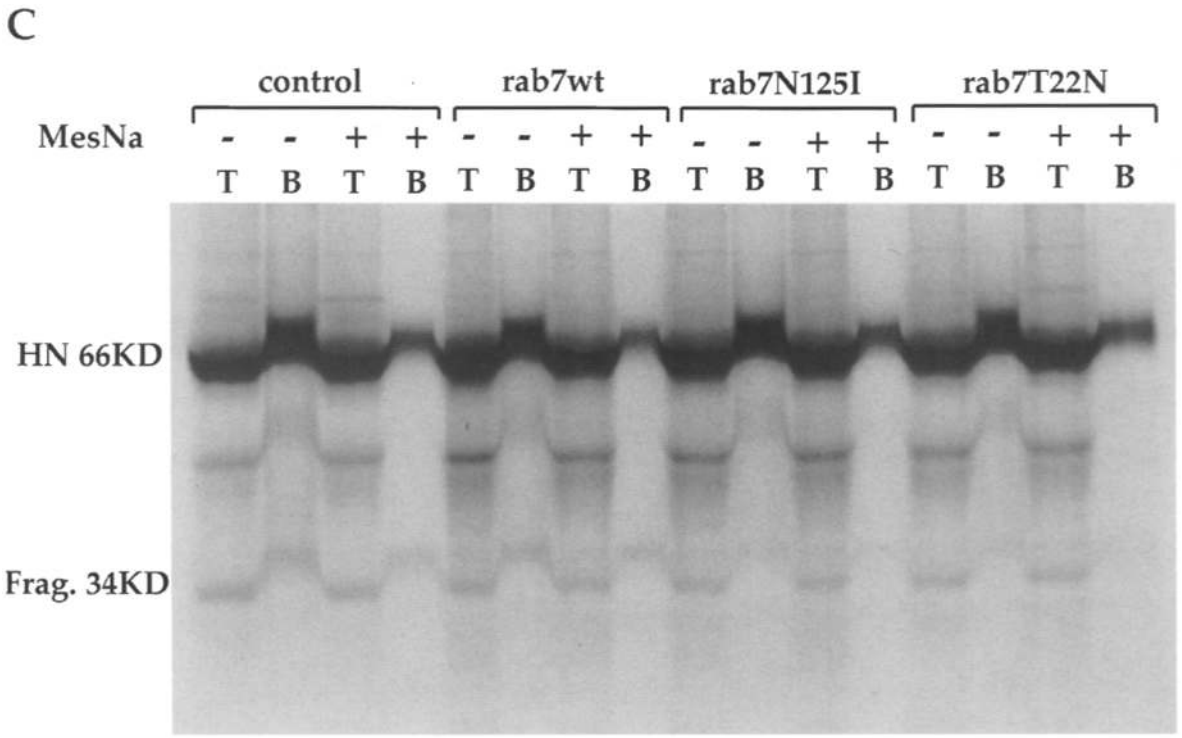

Figure 11. SV5 HN internalization and degradation are differentially affected by dominant negative mutant forms of rab7. SV5 HN was expressed in BHK cells either alone (*control*) or together with wild-type (*rab7wt*), or mutant rab7N125I or rab7T22N proteins, as described in Materials and Methods. SV5 HN was pulse-labeled with [^{35}S]methionine and allowed to reach the cell surface during a 1-h incubation at 37°C. Cell surface proteins, including SV5 HN, were modified with sulfo-NHS-SS-biotin at 4°C as detailed in the Materials and Methods. Cells were then returned to 37°C for 1 h to allow internalization of the biotin-labeled HN. One group of duplicate samples was then incubated with the reducing agent MESNA (+), while a second group was left untreated (−). See Materials and Methods for details. (*A*) Percentages of internalized, biotinylated HN quantified using a Fuji Bioimager. Each bar and associated SD is representative of three independent trials. (*B*) Percentages of cleaved HN quantified using a Fuji Bioimager and calculated using the formulas described in Materials and Methods. Each bar and associated SD is representative of three independent trials. (*C*) A representative autoradiograph used for the quantification shown in *A–B*. SV5 HN was recovered from cell lysates by immunoprecipation with a specific anti-SV5 HN monoclonal, 1b. One-fifth of each immunoprecipitated sample was analyzed directly by SDS-PAGE using 10% gels (*T* lanes), the remainder of each sample was treated with streptavidin-agarose to recover the biotinylated HN (*B* lanes) before analysis by SDS-PAGE. The large amount of immunoglobulin present in the *T* lanes is responsible for the increased mobility of all bands in these lanes. After electrophoresis, the gel was subjected to autoradiography. Intact SV5 HN migrated with an apparent molecular weight of 66 kD and a specific cleavage fragment was detected at 34 kD. A 45-kD band observed most strongly in the immunoprecipitated samples (*T*, −, +) was not internalized (see *B*, + *MESNA* lanes), and therefore was not considered relevant in the evaluation of the experiment.

readily detected at this time point (Fig. 11 *C*, *Frag. 34 kD*). The cleavage product was not formed in control cells maintained at 4°C indicating that internalization is required for cleavage (data not shown). Quantification of three independent trials revealed that HN internalization was similar irrespective of whether wild-type rab7 or the mutants rab7N125I or rab7T22N were overexpressed (Fig. 11 *A*). The percentages of HN internalized in all cases were similar to mock-transfected controls (Fig. 11 *A*, *control*). The situation was different when the degradation of HN was quantified. Overexpression of rab7N125I or rab7T22N decreased the degradation of HN by 50% at the 60-min time point (Fig. 11 *B*). The percentage of HN degraded in cells overexpressing wild-type rab7 was similar to that measured in mock-transfected control cells. These assays, using two different markers, confirm that rab7 has no influence on early endocytic events including internalization, but rather affects transport to late endosomes where degradation is initiated.

Discussion

In this study, we demonstrate that rab7 is functionally distinct from rab5 and rab9, serving to regulate transport from early to late endosomes. This was accomplished by transiently overexpressing the wild-type rab7 or mutant rab7N125I and rab7T22N proteins, and subsequently monitoring their effects on exocytosis and various stages of endocytosis. Both mutant proteins behaved as dominant negative inhibitors of membrane transport from early to late endosomes. Their overexpression resulted in an accumulation of the transport marker, VSV G protein, in early endosomes and reduced the late endocytic cleavage of SV5 HN by 50% as compared to mock-transfected cells and cells overexpressing wild-type rab7 protein. The finding that the mutant proteins did not completely block transport to late endosomes is consistent with other studies using mutant rab proteins which generally decreased the rate of any single membrane transport step under in-

vestigation between 50 and 66% (Bucci et al., 1992; Martinez et al., 1994; Stenmark et al., 1994). On the other hand, the mutant proteins had no apparent effect on early internalization events known to be regulated by rab5 (Barbieri et al., 1994; Bucci et al., 1992; Gorvel et al., 1991; Li and Stahl, 1993). Both the transport of VSV G protein to early endosomes in cells incubated at 15°C and the short-term internalization of HRP were unchanged by the presence of the mutant proteins.

Parallel findings have been reported in the yeast system where Ypt51p, Ypt52p, Ypt53p, and Ypt7p are thought to be functional homologues of the mammalian rab5a, rab5b, rab5c, and rab7 proteins, respectively (Singer-Krüger et al., 1994; Wichmann et al., 1992). Internalization and degradation of the yeast pheromone α-factor were used as a measure of delivery to the vacuole, the principle degradative organelle in yeast. A null *ypt51ypt52ypt53* mutant inhibited internalization (Singer-Krüger et al., 1994). In contrast, a null *ypt7* mutant had no effect on α-factor internalization, but rather delayed its degradation three-fold (Wichmann et al., 1992). This data coupled with the fact that *ypt51ypt52ypt53* and *ypt7* mutants accumulated α-factor in early or late endosomes, respectively, led to the suggestion that Ypt51p, Ypt52p, and Ypt53p function upstream of Ypt7p (Schimmöller and Riezman, 1993; Singer-Krüger et al., 1994). In spite of this similarity some questions remain.

YPT7 was initially described as being required for transport from early to late endosomes in yeast (Wichmann et al., 1992). However, a more recent report has implicated Ypt7p in a later event mediating transport from the late endosome to the vacuole of yeast (Schimmöller and Riezman, 1993). One issue which remains unresolved is whether rab7 might also regulate transport from the late endosomes to lysosomes in mammalian cells. To date, no rab proteins have been found associated with lysosomes yet transport from late endosomes to lysosomes in vitro is blocked by GTPγS, implicating GTPases in this process (Mullock et al., 1994). It is possible that rab7 is important for both transport events. Our current assays cannot exclude this possibility, assuming transport was blocked at the first point of rab7 action upon overexpression of the dominant negative mutant protein. It is also possible that additional rab family GTPases and/or isoforms are involved in late endocytic membrane transport, as has been shown to be the case for early endocytic events. For example, seven rab proteins have been localized to early endosomes (rab5a, b, and c; rab4a and b, rab18 and rab20) and shown to be important for plasma membrane internalization, early endosome fusion, and recycling from the early endosome (Bucci et al., 1992, 1994; Lütcke et al., 1994; Simons and Zerial, 1993; van der Sluijs et al., 1991, 1992).

Two models have been proposed to describe endocytic processes and a large body of supporting data exists for each (Aniento et al., 1993; Dunn and Maxfield, 1992; Gruenberg et al., 1989; Stoorvogel et al., 1991). The "maturation model" proposes that clathrin-coated vesicles formed from the plasma membrane gradually mature to give rise to lysosomes (Dunn and Maxfield, 1992; Helenius et al., 1983; Murphy, 1991). The "vesicle shuttle model" proposes that early and late endosomes and lysosomes are unique compartments interconnected by vesicular membrane transport (Helenius et al., 1983; Ludwig et al., 1991). Our findings favor a model involving vesicular transfer from early to late endosomes. Evidence is presented for the involvement of a rab protein in this step. Rab proteins are known to be key regulators of vesicle budding and fusion events (Bourne, 1988; Nuoffer et al., 1994; Pfeffer, 1994; Pind et al., 1994; Walworth et al., 1989). Therefore, a vesicular intermediate is most likely required. Furthermore, if a "maturation" pathway was inhibited by the dominant negative mutant rab7 proteins, it might be expected to influence the formation of late endosomes and lysosomes and consequently the distribution of associated markers (Dunn and Maxfield, 1992; Ward et al., 1995). No such changes in the steady state distributions of either mannose 6-phosphate receptor (late endosomes) or of lysosomal glycoprotein 120 (lysosomes) were observed up to 2.5 h after the mutant rab7 protein was overexpressed at high levels. Assuming that the time frame analyzed is sufficient for late endosomes and lysosomes to turn over, this finding too would seemingly contradict the maturation model and lend support to the vesicle shuttle model. Analysis of the long-term effects of overexpressing wild-type or mutant forms of rab7 in stable, inducible cell lines (Press, B., and A. Wandinger-Ness, unpublished data) will be useful in shedding further light on this issue.

In summary, rab7 has been shown to be an important regulator of transport to the late endosome. Therefore, it is expected to be an invaluable tool in dissecting late endosome-associated functions. In addition to antigen-processing activities (Benaroch et al., 1995; Qiu et al., 1994; Sanderson et al., 1994), the late endosome has also been implicated in phagocytosis (Desjardins et al., 1994*a*; Desjardins et al., 1994*b*), and pathogen uptake (Beron et al., 1995). It is conceivable that rab7, in combination with the rab5 mutant proteins, and serve as tools to dissect the important intermediates in these pathways and address issues pertaining to their compartmentalization.

We gratefully acknowledge the expert technical assistance provided by Ms. Julie Kaplan-Arey throughout this project, Mr. John Davis for constructing the rab7T22N mutant, and Ms. Mary Slater Venkata for performing the GTP-overlay blots. We extend our thanks to Ms. Karen Ector for technical advice and helpful discussions relating to studies measuring the biotinylation, internalization, and cleavage of SV5 HN. Drs. Marino Zerial and Cecilia Bucci kindly provided us with the cloned rab7 and rab7N125I genes. We also thank Drs. Bernard Hoflack, Jean Gruenberg, Douglas Lyles and Kathryn Howell, Marino Zerial, Suzanne Pfeffer, and Robert Lamb for their kind gifts of antisera. A. Wandinger-Ness extends special thanks to her colleagues for their generosity, support, and advice in the course of her first three years as an assistant professor in the Department of Biochemistry, Molecular Biology and Cell Biology at Northwestern University, especially Drs. Robert Lamb and Richard Morimoto for generously sharing equipment; Richard Gaber, Susan Pierce, Daniel Linzer, and Robert Macdonald for helpful discussions; and Scott Ness for expert advice on molecular biology. We thank Drs. Robert Lamb and Marino Zerial for critical reading of the manuscript.

This work was supported by grants from American Cancer Society, Illinois Division (93-67) and The Council for Tobacco Reseach (3980) to A. Wandinger-Ness. B. Press was supported by a United States Public Health Services Predoctoral Biotechnology Training Grant (T32GM-08449).

Received for publication 5 June 1995 and in revised form 17 July 1995.

References

Aniento, F., N. Emans, G. Griffiths, and J. Gruenberg. 1993. Cytoplasmic dynein-dependent vesicular transport from early to late endosomes. *J. Cell*

Biol. 123:1373–1387.

Barbieri, M. A., G. Li, M. I. Colombo,and P. D. Stahl. 1994. Rab5, an early acting endosomal GTPase, supports in vitro endosome fusion without GTP hydrolysis. *J. Biol. Chem.* 269:18720–18722.

Benaroch, P., M. Yilla, G. Raposo, K. Ito, K. Miwa, H. J. Geuze, and H. L. Ploegh. 1995. How MHC class II molecules reach the endocytic pathway. *EMBO (Eur. Mol. Biol. Organ.) J.* 14:37–49.

Beron, W., C. Alvarez-Dominguez, L. Mayorga, and P. D. Stahl. 1995. Membrane trafficking along the phagocytotic pathway. *Trends Cell. Biol.* 5:100–104.

Bourne, H. R. 1988. Do GTPases direct membrane traffic in secretion? *Cell.* 53: 669–671.

Bourne, H. R., D. A. Sanders, and F. McCormick. 1990. The GTPase superfamily: a conserved switch for diverse cell functions. *Nature (Lond.).* 348:125–132.

Bucci, C., R. G. Parton, I. H. Mather, H. Stunnenberg, K. Simons, B. Hoflack, and M. Zerial. 1992. The small GTPase rab5 functions as a regulatory factor in the early endocytic pathway. *Cell.* 70:715–728.

Bucci, C., A. Wandinger-Ness, A. Lutcke, M. Chiariello, C. b. Bruni, and M. Zerial. 1994. Rab5a is a common component of the apical and basolateral endocytic machinery in polarized epithelial cells. *Proc. Natl. Acad. Sci. USA.* 91:5061–5065.

Chavrier, P., R. G. Parton, H. P. Hauri, K. Simons, and M. Zerial. 1990. Localization of low molecular weight GTP binding proteins to exocytic and endocytic compartments. *Cell.* 62:317–329.

Cresswell, P. 1994. Assembly, transport, and function of MHC class II molecules. *Annu. Rev. Immunol.* 12:259–293.

de Silva, A. M., W. E. Balch, and A. Helenius. 1990. Quality control in the endoplasmic reticulum: folding and misfolding of vesicular stomatitis virus G protein in cells and in vitro. *J. Cell Biol.* 111:857–866.

de Vos, A. M., L. Tong, M. W. Milburn, P. M. Matias, J. Jancarik, S. Noguchi, S. Nishimura, K. Miura E. Ohtsuka, and S. H. Kim. 1988. Three-dimensional structure of an oncogene protein: catalytic domain of human c-H-ras p21. *Science (Wash. DC).* 239:888–893.

Der, C. J., B. T. Pan, and G. M. Cooper. 1986. rasH mutants deficient in GTP binding. *Mol. Cell. Biol.* 6:3291–3294.

Desjardins, M., J. E. Celis, G. van Meer, H. Dieplinger, A. Jahraus, G. Griffiths, and L. A. Huber. 1994*a*. Molecular characterization of phagosomes. *J. Biol. Chem.* 269:32194–32200.

Desjardins, M., L. A. Huber, R. G. Parton, and G. Griffiths. 1994*b*. Biogenesis of phagolysosomes proceeds through a sequential series of interactions with the endocytic apparatus. *J. Cell Biol.* 124:677–688.

Doms, R. W., D. S. Keller, A. Helenius, and W. E. Balch. 1987. Role for adenosine triphosphate in regulating the assembly and transport of vesicular stomatitis virus G protein trimers. *J. Cell Biol.* 105:1957–1969.

Draper, R. K., D. O. O'Keefe, M. Stookey, and J. Graves. 1984. Identification of a cold-sensitive step in the mechanism of modeccin action. *J. Biol. Chem.* 259:4083–4088.

Dunn, K. W., and F. R. Maxfield. 1992. Delivery of ligands from sorting endosomes to late endosomes occurs by maturation of sorting endosomes. *J. Cell Biol.* 117:301–310.

Dunn, W. A., A. L. Hubbard, and N. J. Aroson. 1980. Low temperature selectively inhibits fusion between pinocytic vesicles and lysosomes during heterophagy of 125I-asialofetuin by the perfused rat liver. *J. Biol. Chem.* 255: 5971–5978.

Dunn, W. A., T. P. Connolly, and A. L. Hubbard. 1986. Receptor-mediated endocytosis of epidermal growth factor by rat hepatocytes: receptor pathway. *J. Cell Biol.* 102:24–36.

Feig, L. A., B. T. Pan, T. M. Roberts, and G. M. cooper. 1986. Isolation of ras GTP-binding mutants using an in situ colony-binding assay. *Proc. Natl. Acad. Sci. USA.* 83:4607–4611.

Ferro-Novick, S., and P. Novick. 1993. The role of GTP-binding proteins in transport along the exocytic pathway. *Annu. Rev. Cell Biol.* 9:575–599.

Frech, M., T. A. Darden, L. G. Pdersen, C. K. Foley, P. S. Charifson, M. W. Anderson, and A. Wittinghofer. 1994. Role of glutamine-61 in the hydrolysis of GTP by $p^{21H\text{-}ras}$: and experimental and theoretical study. *Biochemistry.* 33: 3237–3244.

Fuerst, T. R., E. G. Niles, F. W. Studier, and B. Moss. 1986. Eukaryotic transient-expression system based on recombinant vaccinia virus that synthesizes bacteriophage T7 RNA polymerase. *Proc. Natl. Acad. Sci. USA.* 83:8122–8126.

Gallione, C. J., and J. K. Rose. 1985. A single amino acid substitution in a hydrophobic domain causes temperature-sensitive cell-surface transport of a mutant viral glycoprotein. *J. Virol.* 54:374–382.

Germain, R. N. 1994. MHC-dependent antigen processing and peptide presentation: providing ligands for T lymphocyte activation. *Cell.* 76:287–299.

Goldstein, J. L., M. S. Brown, R. G. Anderson, D. W. Russell, and W. J. Schneider. 1985. Receptor-mediated endocytosis: concepts emerging from the LDL receptor system. *Annun. Rev. Cell Biol.* 1:1–39.

Gorvel, J. P., P. Chavrier, M. Zerial, and J. Gruenberg. 1991. rab5 controls early endosome fusion in vitro. *Cell.* 64:915–925.

Griffiths, G., R. Matteoni, R. Back, and B. Hoflack. 1990. Characterization of the cation-independent mannose 6-phosphate receptor-enriched prelysosomal compartment in NRK cells. *J. Cell Sci.* 95:441–461.

Gruenberg, J., G. Griffiths, and K. E. Howell. 1989. Characterization of the early endosome and putative endocytic carrier vesicles in vivo and with an assay of vesicle fusion in vitro. *J. Cell. Bio.* 108:1301–1316.

Harter, C., and I. Mellman. 1992. Transport of the lysosomal membrane glycoprotein lgp120 (lgp-A) to lysosomes does not require appearance on the plasma membrane. *J. Cell Biol.* 117:311–325.

Helenius, A., I. Mellman, D. Wall, and A. Hubbard. 1983. Endosomes. *Trends Biochem. Sci.* 8:245–250.

Honing, S., and W. Hunziker. 1995. Cytoplasmic determinants involved in direct lysosomal sorting, endocytosis, and basolateral targeting of rat lgp120 (lamp-I) in MDCK cells *J. Cell Biol.* 128:321–332.

Huber, L. A., S. Pimplikar, R. G. Parton, H. Virta, M. Zerial, and K. Simons. 1993. Rab8, a small GTPase involved in vesicular traffic between the TGN and the basolateral plasma membrane. *J. Cell Biol.* 123:35–45.

John, J., H. Rensland, I. Schlichting, I. Vetter, G. D. Borasio, R. S. Goody, and A. Wittinghofer. 1993. Kinetic and structural analysis of the Mg^{2+}-binding site of the guanine nucleotide-binding protein $p^{21H\text{-}ras}$. *J. Biol. Chem.* 268: 923–929.

Jurnak, F., S. Heffron, and E. Bergmann. 1990. Conformational changes involved in the activation of ras p21: implications for related proteins. *Cell.* 60: 525–528.

Klumperman, J., A. Hille, T. Veenendaal, V. Oorschot, W. Stoorvogel, K. von Figura, and H. J. Geuze. 1993. Differences in the endosomal distributions of the two mannose 6-phosphate receptors. *J. Cell Biol.* 121:997–1010.

Kreis, T. E., and H. F. Lodish. 1986. Oligomerization is essential for transport of vesicular stomatitis viral glycoprotein to the cell surface. *Cell.* 46:929–937.

Lefrancios, L., and D. S. Lyles. 1982. The interaction of antibody with the major surface glycoprotein of vesicular stomatitis virus. I. Analysis of neutralizing epitopes with monoclonal antibodies. *Virology.* 121:157–167.

Leser, G. P., K. J. Ector, and L. A. Lamb. 1996. The paramyxovirus SV5 HN glycoprotein, but not the F glycoprotein is internalized via coated pits and enters the endocytic pathway. *Mol. Biol. Cell.* In press.

Li, G., and P. D. Stahl. 1993. Structure-function relationship of the small GTPase rab5. *J. Biol. Chem.* 268:24475–24480.

Li, G., M. A. Barbieri, M. I. Colombo, and P. D. Stahl. 1994. Structural features of the GTP-binding defective Rab5 mutants required for their inhibitory activity on endocytosis. *J. Biol. Chem.* 269:14631–14635.

Lombardi, D., T. Soldati, M. A. Riederer, Y. Goda, M. Zerial, and S. R. Pfeffer. 1993. Rab9 functions in transport between late endosomes and the *trans* Golgi network. *EMBO (Eur. Mol. Biol. Organ.) J.* 12:677–682.

Ludwig, T., G. Griffiths, and B. Hoflack. 1991. Distribution of newly synthesized lysosomal enzymes in the endocytic pathway of normal rat kidney cells. *J. Cell Biol.* 115:1561–1572.

Lütcke, A., R. G. Parton, C. Murphy, V. Olkkonen, P. Dupree, A. Valencia, K. Simons, and M. Zerial. 1994. Cloning and subcellular localization reveals polarized and cell type-specific expression. *J. Cell Sci.* 107:3437–3448.

Martinez, O., A. Schmidt, J. Salamero, B. Hoflack, M. Roa, and B. Goud. 1994. The small GTP-binding protein rab6 functions in intra-Golgi transport. *J. Cell Biol.* 127:1575–1588.

Milburn, M. V., L. Tong, A. M. deVos, A. Brunger, Z. Yamaizumi, S. Nishimura, and S. H. Kim. 1990. Molecular switch for signal transduction: structural differences between active and inactive forms of protooncogenic ras proteins. *Science (Wash. DC)* 247:939–945.

Mullock, B. M., J. H. Perez, T. Kuwana, S. R. Gray, and J. P. Luzio. 1994. Lysosomes can fuse with a late endosomal compartment in a cell-free system from rat liver. *J. Cell Biol.* 126:1173–1182.

Murphy, R. 1991. Maturation models for endosome and lysosome biogenesis. *Trends Cell Biol.* 1:77–82.

Ng, D. T., R. E. Randall, and R. A. Lamb. 1989. Intracellular maturation and transport of the SV5 type II glycoprotein hemagglutinin-neuraminidase: specific and transient association with GRP78-BiP in the endoplasmic reticulum and extensive internalization from the cell surface. *J. Cell Biol.* 109:3273–3289.

Novick, P., and P. Brennwald. 1993. Friends and family: the role of the Rab GTPases in vesicular traffic. *Cell.* 75:597–601.

Nuoffer, C., H. W. Davidson, J. Matteson, J. Meinkoth, and W. E. Balch. 1994. A GDP-bound of rab1 inhibits protein export from the endoplasmic reticulum and transport between Golgi compartments. *J. Cell. Biol.* 125:225–237.

Oka, J. A., and P. H. Weigel. 1983. Microtubule-depolymerizing agents inhibit asialo-orosomucoid delivery to lysosomes but not its endocytosis or degradation in isolated rat hepatocytes. *Biochim. Biophys. Acta.* 763:368–376.

Olkkonen, V. M., P. Dupree, I. Killisch, A. Lütcke, M. Zerial, and K. Simons. 1993. Molecular cloning and subcellular localization of three GTP-binding proteins of the rab subfamily. *J. Cell Sci.* 106:1249–1261.

Pai, E. F., W. Kabsch, U. Krengel, K. C. Holmes, J. John, and A. Wittinghofer. 1989. Structure of the guanine-nucleotide-binding domain of the Ha-ras oncogene product p21 in the triphosphate conformation. *Nature (Lond.).* 341: 209–214.

Paterson, R. G., S. W. Hiebert, and R. A. Lamb. 1985. Expression at the cell surface of biologially active fusion and hemagglutinin/neuraminidase proteins of the paramyxovirus simian virus 5 from cloned cDNA. *Proc. Natl. Acad. Sci. USA.* 82:7520–7524.

Pfeffer, S. R. 1994. Rab GTPases: master regulators of membrane trafficking. *Curr. Opin. Cell Biol.* 6:522–526.

Pind, S. N., C. Nuoffer, J. M. McCaffery, H. Plutner, H. W. Davidson, M. G. Farquhar, and W. E. Balch. 1994. Rab1 and Ca^{2+} are required for the fusion

of carrier vesicles mediating endoplasmic reticulum to Golgi transport. *J. Cell Biol.* 125:239–252.

Plutner, H., A. D. Cox, S. Pind, R. Khosravi-Far, J. R. Bourne, R. Schwaninger, C. J. Der, and W. E. Balch. 1991. Rab1b regulates vesicular transport between the endoplasmic reticulum and successive Golgi compartments. *J. Cell Biol.* 115:31–43.

Qiu, Y., X. Xu, A. Wandinger-Ness, D. P. Dalke, and S. K. Pierce. 1994. Separation of subcellular compartments containing distinct functional forms of MHC class II. *J. Cell Biol.* 125:595–605.

Rabinowitz, S., H. Horstmann, S. Gordon,and G. Griffiths. 1992. Immunocytochemical characterization of the endocytic and phagolysosomal compartments in peritoneal macrophages. *J. Cell Biol.* 116:95–112.

Randall, R. E., D. F. Young, K. K. Goswami, and W. C. Russell. 1987. Isolation and characterization of monoclonal antibodies to simian virus 5 and their use in revealing antigenic differences between human, canine and simian isolates. *J. Gen. Virol.* 68:2769–2780.

Riederer, M. A., T. Soldati, A. D. Shapiro, J. Lin, and S. R. Pfeffer. 1994. Lysosome biogenesis requires Rab9 function and receptor recycling from endosomes to the *trans*-Golgi network. *J. Cell Biol.* 125:573–582.

Salminen, A., and P. J. Novick. 1987. A ras-like protein is required for a post-Golgi event in yeast secretion. *Cell* 49:527–538.

Sanderson, F., M. J. Kleijmeer, A. Kelly, D. Verwoerd, A. Tulp, J. J. Neefjes, H. J. Geuze, and J. Trowsdale. 1994. Accumulationof HLA-DM, a regulator of antigen presentation, in MHC class II compartments. *Science (Wash. DC).* 266:1566–1569.

Schimmöller, F., and H. Riezmann. 1993. Involvement of Ypt7p, a small GTPase, in traffic from late endosome to the vacuole in yeast. *J. Cell Sci.* 106:823–830.

Schlichting, I., S. C. Almo, G. Rapp, K. Wilson, K. Petratos, A. Lentfer, A. Wittinghofer, W. Kabsch, E. F. Pai, G. A. Petsko, et al. 1990. Time-resolved X-ray crystallographic study of the conformational change in Ha-Ras p21 protein on GTP hydrolysis. *Nature (Lond).* 345:309–315.

Segev, N. 1991. Mediation of the attachment or fusion step in vesicular transport by the GTP-binding Ypt1 protein. *Science (Wash. DC).* 252:1553–1556.

Segev, N., J. Mulholland, and D. Botstein. 1988. The yeast GTP-binding YPT1 protein and a mammalian counterpart are associated with the secretion machinery. *Cell.* 52:915–924.

Sigal, I. S., J. B. Gibbs, J. S. D'Alonzo, G. L. Temeles, B. S. Wolanski, S. H. Socher, and E. M. Scolnick. 1986. Mutant ras-endcoded proteins with altered nuclotide binding exert dominant biological effects. *Proc. Natl. Acad. Sci. USA.* 83:952–956.

Simons, K., and M. Zerial. 1993. Rab proteins and the road maps for intracellular transport. *Neuron.* 11:789–799.

Singer-Krüger, B., H. Stenmark, A. Dusterhoft, P. Philippsen, J. S. Yoo, D. Gallwitz, and M. Zerial. 1994. Role of three rab5-like GTPases, Ypt51p, Tpt52p, and Ypt53p, in the endocytic and vacuolar protein sorting pathways of yeast. *J. Cell Biol.* 125:283–298.

Smythe, E., T. E. Redelmeier, and S. L. Schmid. 1992. Receptor-mediated endocytosis in semi-intact cells. *Methods Enzymol.* 219:223–234.

Stenmark, H., R. G. Parton, O. Steele-Mortimer, A. Lutcke, J. Gruenberg, and M. Zerial. 1994. Inhibition of rab5 GTPase activity stimulates membrane fusion in endocytosis. *EMBO (Eur. Mol. Biol. Organ.) J.* 13:1287–1296.

Stoorvogel, W., G. J. Stous, H. J. Geuze, V. Oorschot, and A. L. Schwartz. 1991. Late endosomes derive from early endosomes by maturation. *Cell.* 65:417–427.

Tisdale, E. J., J. R. Bourne, R. Khosravi-Far, C. J. Der, and W. E. Balch. 1992. GTP-binding mutants of rab1 and rab2 are potent inhibitors of vesicular transport from the endoplasmic reticulum to the Golgi complex. *J. Cell Biol.* 119:749–761.

Tong, L. A., A. M. de Vos, M. V. Milburn, J. Jancarik, S. Noguchi, S. Nishimura, K. Miura, E. Ohtsuka and S. H. Kim. 1989. Structural differences between a ras oncogene protein and the normal protein. *Nature (Lond.).* 337: 90–93.

van der Sluijs, P., M. Hull, A. Zahraoui, A. Tavitian, B. Goud, and I. Mellman. 1991. The small GTP-binding protein rab4 is associated with early endosomes. *Proc. Natl. Acad. Sci. USA.* 88:6313–6317.

van der Sluijs, P., M. Hull, P. Webster, P. Male, B. Goud, and I. Mellman. 1991. The small GTP-binding protein rab4 controls an early sorting event on the endocytic pathway. *Proc. Natl. Acad. Sci. USA.* 70:729–740.

Walworth, N. C., B. Goud, A. K. Kabcenell, and P. J. Novick. 1989. Mutational analysis of SEC4 suggests a cyclical mechanism for the regulation of vesicular traffic. *EMBO (Eur. Mol. Biol. Organ.) J.* 8:1685–1693.

Ward, D. M., C. M. Perou, M. Lloyd,, and J. Kaplan. 1995. "Synchronized" endocytosis and intracellular sorting in alveolar macrophages: the early sorting endosome is a transient organelle. *J. Cell Biol.* 129:1229–1240.

Whitt, M. A., L. Chong, and J. K. Rose. 1989. Glycoprotein cytoplasmic domain sequences required for rescue of a vesicular stomatitis virus glycoprotein mutant. *J. Virol.* 63:3569–3578.

Wichmann, H., L. Hengst, and D. Gallwitz. 1992. Endocytosis in yeast: evidence for the involvement of a small GTP-binding protein (Ypt7p). *Cell.* 71: 1131–1142.

Yamashiro, D. J., B. Tycko, S. R. Fluss, and F. R. Maxfield. 1984. Segregation of transferrin to a mildly acidic (pH 6.5) para-Golgi compartment in the recycling pathway. *Cell.* 37:789–800.

Zerial, M., and H. Stenmark. 1993. Rab GTPase in vesicular transport. *Curr. Opin. Cell Biol.* 5:613–620.